
[All ETDs from UAB](#)

[UAB Theses & Dissertations](#)

2005

Electrolytic deposition of calcium phosphates on modified titanium substrates.

Rebecca Shumate O'Connor Davis
University of Alabama at Birmingham

Follow this and additional works at: <https://digitalcommons.library.uab.edu/etd-collection>

Recommended Citation

Davis, Rebecca Shumate O'Connor, "Electrolytic deposition of calcium phosphates on modified titanium substrates." (2005). *All ETDs from UAB*. 5400.
<https://digitalcommons.library.uab.edu/etd-collection/5400>

This content has been accepted for inclusion by an authorized administrator of the UAB Digital Commons, and is provided as a free open access item. All inquiries regarding this item or the UAB Digital Commons should be directed to the [UAB Libraries Office of Scholarly Communication](#).

ELECTROLYTIC DEPOSITION OF CALCIUM PHOSPHATES ON MODIFIED
TITANIUM SUBSTRATES

by

REBECCA SHUMATE O'CONNOR DAVIS

A DISSERTATION

Submitted to the graduate faculty of The University of Alabama at Birmingham,
in partial fulfillment of the requirements for the degree of
Doctor of Philosophy

BIRMINGHAM, ALABAMA

2005

UMI Number: 3187857

Copyright 2005 by
Davis, Rebecca Shumate O'Connor

All rights reserved.

INFORMATION TO USERS

The quality of this reproduction is dependent upon the quality of the copy submitted. Broken or indistinct print, colored or poor quality illustrations and photographs, print bleed-through, substandard margins, and improper alignment can adversely affect reproduction.

In the unlikely event that the author did not send a complete manuscript and there are missing pages, these will be noted. Also, if unauthorized copyright material had to be removed, a note will indicate the deletion.

UMI[®]

UMI Microform 3187857

Copyright 2006 by ProQuest Information and Learning Company.

All rights reserved. This microform edition is protected against
unauthorized copying under Title 17, United States Code.

ProQuest Information and Learning Company
300 North Zeeb Road
P.O. Box 1346
Ann Arbor, MI 48106-1346

Copyright by
Rebecca Shumate O'Connor Davis
2005

ABSTRACT OF DISSERTATION
GRADUATE SCHOOL, UNIVERSITY OF ALABAMA AT BIRMINGHAM

Degree Ph.D. Program Materials Science
Name of Candidate Rebecca Shumate O'Connor Davis
Committee Chair Gregg M. Janowski
Title Electrolytic Deposition of Calcium Phosphates on Modified Titanium Substrates

Orthopedic and dental implants are often coated with calcium phosphate (CaP) to promote better bonding between bone and implant. Plasma spraying is used for most CaP coatings, although these coatings can fail due to high internal stresses created by the thermal mismatch. The high temperatures reached in plasma spraying also causes multiple CaP phases to occur within the coating, leading to areas of the coating being resorbed more quickly than others. Other coating techniques have been developed to overcome these limitations of plasma spraying and to improve overall CaP coating performance.

Electrolytic deposition (ELD) is a novel technique that has shown promise as a low temperature alternative. ELD is a non-line-of-sight technique capable of depositing thin CaP coatings. The coating deposition can be controlled by adjustment of the current, temperature, bath composition, and pH.

The objective of this research was to develop a system using ELD to deposit CaP coatings of desired solubilities on commercially pure titanium with good bond strengths. The titanium was either passivated nitric acid (NPAS) or treated further with phosphoric acid (PMOD) to determine if the surface chemistry change improved ELD or coating bond strength. A resorbable CaP composed of predominantly octacalcium phosphate (OCP) and hydroxylapatite (HA) was deposited using a constant current applied through an unbuffered CaP electrolyte at 37°C. The bath chemistry was adjusted using the Gibb's

free energy calculated from the solubility isotherms of the CaP system to deposit HA. A square wave was used to apply the ELD HA coatings. ELD HA and sintered HA pellets were incubated in biological saline over a 14 day period and were found to draw Ca and P from solution onto the surfaces. Both the ELD resorbable CaP and ELD HA coatings had high bond strengths to the substrates, regardless of surface treatment. The ELD HA coatings were seeded with human mesenchymal stem cells (MSC) with and without serum present. MSC required serum for the cells to spread on all surfaces. Cell spreading occurred within the first hour, and cytoskeleton and actin fibers were visible at 24 hours. ELD of CaP shows promise as an affordable, low-temperature process for further development toward use as a coating technique for biomedical implants.

DEDICATION

To Michael and Mom.

ACKNOWLEDGEMENTS

There are many people without whom this dissertation would not have come to completion, and I could never be able to properly thank each and every one for their assistance. First, I thank my research mentor Dr. Gregg M. Janowski, who has worn many hats throughout this process: program director, advisor, and editor, to name a few. His constant support, guidance, and willingness to take on the challenges presented by this research kept me motivated throughout. I thank Dr. Ramakrishna Venugopalan who provided initial shaping of the project and financial support for this research. Many thanks also go to the remaining members of my committee - Drs. Susan L. Bellis, Linda C. Lucas, Garry Warren, and Giovanni Zangari - for their time, support and input as the project progressed. I thank Dr. William R. Lacefield for fostering my initial interest in calcium phosphates and his continued support and valuable suggestions even after his retirement.

The collection and analysis of much of this data would not have been possible without the assistance of several people. Being a student in the Materials Science program afforded me the opportunity to collaborate with many people throughout the state of Alabama. Many thanks to Ms. Cheri Moss and Dr. Robin Griffin for training me to use the scanning electron microscope and electron dispersive spectroscopy system at UAB. I also thank Dr. Earl Ada of the University of Alabama, Tuscaloosa, for training me on the X-ray photoelectron spectrometer and helping with the analysis of the obtained spectra. My gratitude goes to Ms. Amber Sawyer for her invaluable help with the cell culture studies. I thank her for providing me with a protocol for my cell experiments, training me

how to execute the protocol, and for taking the images of my cells on the fluorescent microscope. I also thank Mr. Ed Calvert of Wallace State Community College for allowing me such open access to learn how to use the inductively coupled plasma-optical emission spectrometer; he truly made me feel welcome in his laboratory. I thank Dr. Derrick Dean and his students for the collection of data on his Fourier transform infrared spectrometer and to Dr. Krishnan Chittur at The University of Alabama in Huntsville for his help with interpretation and analysis of the spectra. I also thank Dr. Ed Walsh who kindly gave his time to help me troubleshoot my electrochemical cell setup and answer any question I had! I thank Drs. Eileen Burke and Jeannie Haman for introducing me to the constant composition calcium phosphate system and teaching me how to use and apply the KS2.bas software.

Thanks also go to all of the support staff across the programs, without whom the departments would be greatly hurting. For administrative help, I am grateful to: Lyn Lewis, Donnette Parks, and Dr. Zoe Dwyer in the School of Engineering, Debbie Hays and Thyrsa Johnson in Biomedical Engineering, and Cynthia Barham and Janice Johnson in Materials Science and Engineering. I also thank Tommy Foley and the rest of the IT group for keeping the computers running and for their help with the link-up to my well-dispersed committee.

Last, but not least, I thank my friends and family who provided technical support, moral support, or some combination of the two over the years. First and foremost, I must thank my dear husband, Michael, for his unwavering love, support, and friendship, as well as for his expertise with all things Microsoft; I would never have achieved this goal without him! I thank my many office and lab mates in the Biomaterials laboratories over

the years that have leant a sympathetic ear and helped with brainstorming: Krista Speer Kilpadi, Regina Messer, Don Petersen, Barb Blum, Hallie Placko Brinkerhuff, Mindi Newman, Marcus Scott, Steve Summy, Andrea Holton, Latisha Salaam, Kim Bailey, Tina Advincula, and Amber Jennings. I also thank my “other officemates” in the Materials department Brad Bingert, Haibin Ning, Selvum Brian Pillay, for allowing me to randomly commandeer their desks when needed and always helping me laugh. Warm thanks go to some special friends that I have had the pleasure to make in my time at UAB: Preston Scarber, Deepak Kilpadi, Dan Heuer, Greg Turner, Shatry Akella, Lashawnda Harris, Mitch Mansfield, and Eric Cheek. To Lilly Harris, Hue Linh Tran, Ginny Smith, Jamie Turner, Caryne Mesquita, Jayne Poole, Huey Gardner, and the “Wednesday women” of St. Mary’s, I thank them all for their continued friendships, support, prayers, and laughter over all of these years. Finally, I thank my mom for her example in attaining her education and for planting the seed for me to believe that I can do anything I set my mind to! And I thank my grandparents, Tom and Shug, and the rest of my family for never letting me forget it!

TABLE OF CONTENTS

	<i>Page</i>
ELECTROLYTIC DEPOSITION OF CALCIUM PHOSPHATES ON MODIFIED TITANIUM SUBSTRATES	i
ABSTRACT OF DISSERTATION	iii
DEDICATION	v
ACKNOWLEDGEMENTS	vi
LIST OF TABLES	xi
LIST OF FIGURES	xii
LIST OF ABBREVIATIONS	xvi
INTRODUCTION	1
Calcium Phosphates	1
Processing	3
Plasma Sprayed Calcium Phosphate Coating	3
Alternate Coating Techniques	4
Substrate Modification	6
Coating Performance	7
Coating Adhesion	7
Cell Adhesion	7
Proposed Study	8
Specific Aims	9
ELECTROLYTIC DEPOSITION OF A RESORBABLE CALCIUM PHOSPHATE COATING	11
ELECTROLYTIC DEPOSITION OF HYDROXYLAPATITE USING A PULSED WAVE TECHNIQUE	38
DISSOLUTION AND CELLULAR BEHAVIOR OF ELECTROLYTICALLY DEPOSITED HYDROXYLAPATITE	62
OVERALL RESULTS AND DISCUSSION	82
Substrate Treatment Effects	82

TABLE OF CONTENTS (Continued)

	<i>Page</i>
Electrolytic Deposition Coating Method	83
Resorbable Calcium Phosphate Coatings	83
Nonresorbable Calcium Phosphate Coatings.....	85
Solubility in Earle's Balanced Salt Solution.....	86
Cell Culture.....	87
CONCLUSIONS.....	93
FUTURE WORK.....	96
LIST OF GENERAL REFERENCES	97

<i>Table</i>	LIST OF TABLES	<i>Page</i>
INTRODUCTION		
1	Listing of common calcium phosphates and relative CaP solubilities.....	2
2	Summary of factors influencing dissolution rate of ceramic coatings.....	4
ELECTROLYTIC DEPOSITION OF A RESORBABLE CALCIUM PHOSPHATE COATING		
1	Comparison of coating adhesion values	23
ELECTROLYTIC DEPOSITION OF HYDROXYLAPATITE USING A PULSED WAVE TECHNIQUE		
1	Summary of cathodic reactions during ELD of CaP.	42
RESULTS AND DISCUSSION		
1	Reactions involving hydroxyl groups at the Ti cathode in a CaP electrolyte.....	84

LIST OF FIGURES

<i>Figure</i>	<i>Page</i>
ELECTROLYTIC DEPOSITION OF A RESORABLE CALCIUM PHOSPHATE COATING	
1	Electrochemical deposition cell showing major components.....29
2	Representative photomicrographs of coatings deposited at various current densities. Below the optimum current density of 150mA/cm ² coatings were discontinuous (a), while those deposited at higher current densities were subject to spalling (c) and (d).....30
3	SEM micrographs of coated substrates after sonication in methanol. More nucleation sites remain on the PMOD surface (b) and (d) than on the NPAS surface (a) and (c).31
4	Micrographs of as deposited coatings deposited at either 100 or 150 mA/cm ² . PMOD coatings exhibited better crystal definition at lower current density (b), but the distinction was lost at higher deposition currents (d).....32
5	SEM micrograph of profile of coating on NPAS surface (a) and PMOD surface(b).33
6	XRD scan of as-deposited ELD CaP coating on NPAS (top) and PMOD (bottom) titanium substrates33
7	Representative XRD scan of as-deposited ELD CaP coating on NPAS with corresponding ICDD files.34
8	Bond strength of ELD CaP coated titanium deposited at different current densities.....35
9	Representative images of coating surface (a) and corresponding stud surface (b) after adhesion test.....35
10	Bond strength of ELD CaP coating (150 mA/cm ² deposition current density).....36
11	Cumulative change in solute calcium (left) and phosphorous (right) content over 14 day dissolution period.....36

LIST OF FIGURES (Continued)

<i>Figure</i>	<i>Page</i>
12 CaP Coatings after 14 days in Earle's Balanced Salt Solution on NPAS (a) and PMOD (b) treated substrates.....	37
13 XRD of CaP coatings after 14 days in EBSS	37
ELECTROLYTIC DEPOSITION OF HYDROXLAPATITE USING A PULSED WAVE TECHNIQUE	
1 Electrochemical deposition cell showing major components.....	54
2 Representation of applied current for pulse deposition experiments. Periods were between 0.1 s (10 Hz) and 2.0 s (0.5 Hz). The maximum and minimum current densities ranged from 196 to 200 mA/cm ² and 0 to 4 mA/cm ² , respectively.	55
3 XRD Spectra of uncoated NPAS and PMOD cpTi substrates show agreement with ICDD file 5-682 for titanium having a (0 0 2) texture.....	56
4 Representative SEM image of ELD CaP coating deposited using constant current density (200 mA/cm ² on NPAS cpTi substrate).....	57
5 Schematic of reaction at cathode.	57
6 ELD coatings on NPAS substrates deposited at different frequencies. A continuous coating was deposited using 2 Hz square wave. Calibration mark is 25µm.	58
7 ELD coated cpTi NPAS (a) and PMOD (b) after placing in an ultrasonic cleaner with methanol for 2 minutes. There are more visible nucleation sites on the ELD PMOD surface.....	59
8 Edge of ELD coating on Ti substrate illustrating coating thickness.....	59
9 XRD spectra of as-deposited ELD HA coatings on ELD NPAS and PMOD cpTi substrates compared to ICDD files and bulk HA (HAU and HAS)	60
10 FTIR spectra reflects similarities between the ELD deposited coatings on cpTi and pressed HA pellets.	61

LIST OF FIGURES (Continued)

<i>Figure</i>	<i>Page</i>
ELECTROLYTIC DEPOSITION OF HA COATINGS: SOLUBILITY AND CELL PROLIFERATION	
1	Schematic of solubility isotherms of CaP phases at 37°C and 0.10 M ionic activity. Republished with the permission of the International and American Associations for Dental Research, from Johnsson ⁷ ; permission conveyed through Copyright Clearance Center, Inc.76
2	ICP Cumulative graphs of Ca and P coming out of solution and onto HA surfaces over a 14 day period.....77
3	SEM images of ELD HA before (a) and after 14 days in EBSS (b).....77
4	Representative XRD spectra of samples before (HA PMOD and HA NPAS) and after dissolution (HA PMOD-14 and HA NPAS-14) compared to ICDD files for HA (9-432) and titanium (5-682).78
5	FTIR spectra of samples before and after 14 day solubility study in EBSS.....79
6	MSC on surfaces after 1 h of incubation. Surfaces were either coated with serum or left uncoated before cell seeding. Serum was required for cells to spread on all surfaces.80
7	MSC on surfaces after 24 h incubation. Stress fibers are visible at this time period on ELD HA surfaces coated with serum while cells on ELD HA surfaces not coated with serum were rounded. Interestingly, in contrast to ELD HA coated materials, uncoated NPAS and PMOD Ti surfaces were able to promote spreading in the absence of adsorbed serum factors.81

RESULTS AND DISCUSSION

1	ELD coated surfaces after 2 minutes in ultrasonic bath of methanol. Coatings are still present on the Ti, but there are more nucleation sites on the PMOD surfaces.89
2	CaP solubility isotherms as applied to the systems used in this study. Negative log of the product of total molar calcium and phosphorous content plotted versus pH. Adapted from Johnsson. ¹⁸ Republished with the permission of the International and American Associations for Dental Research; permission conveyed through Copyright Clearance Center, Inc.90
3	Phase stability of the resorbable CaP electrolyte system (Ca and P molar concentrations held constant, equal to 6.1×10^{-4} M).91

LIST OF FIGURES (Continued)

<i>Figure</i>	<i>Page</i>
4 Schematic representing the reactions at the cathode surface during ELD of CaP.....	91
5 Phase stability of the nonresorbable CaP electrolyte system (Ca and P molar concentrations held constant, $[Ca] = 1.0 \times 10^{-4} \text{ M}$, $[P] = 6.0 \times 10^{-4} \text{ M}$).	92

LIST OF ABBREVIATIONS

CaP	calcium phosphate
cpTi	commercially pure titanium
DCPA	dicalcium phosphate anhydrous
DCPD	dicalcium phosphate dihydrate
EBSS	Earle's Balanced Salt Solution
EDS	Electron Dispersive Spectroscopy
ELD	electrolytic deposition
FTIR	Fourier Transform Infrared Spectroscopy
HA	hydroxylapatite
HAS	sintered hydroxylapatite pellet
HAU	unsintered hydroxylapatite pellet
ICP	Inductively Coupled Plasma
ICDD	International Centre for Diffraction Data
MSC	mesenchymal stem cells
NPAS	nitric acid passivated
OCP	octacalcium phosphate
PBS	phosphate buffered saline
PMOD	phosphoric acid modified
PS	plasma spray
SEM	Scanning Electron Microscopy

LIST OF ABBREVIATIONS (Continued)

TBS	Tris-buffered saline
TCP	tricalcium phosphate
TTCP	tetracalcium phosphate
XPS	X-ray Photoelectron Spectroscopy
XRD	X-ray Diffraction

INTRODUCTION

Calcium Phosphates

Calcium phosphates (CaP) are biocompatible, surface-reactive ceramics that can attach to bone directly through bioactive fixation.¹ CaP have been used as coatings for approximately 20 years in dentistry and orthopedics, exploiting the chemical properties of the ceramic in combination with the mechanical properties of the substrate.²⁻⁴ CaP coatings have been shown to facilitate early bone integration for implants, as well as exhibit osteoconductive properties in stable and unstable mechanical conditions.⁵⁻⁹ It has been found that the strength of CaP coatings is improved at a thickness under 100 μm .¹⁰ Implants with CaP coatings in the range of 20-50 μm and as thin as 2-4 μm still show improved bone apposition compared to other non-coated cementless implants.^{10,11} The bonding mechanism between the coating and bone involves a sequence of reactions that include dissolution, precipitation, and ion exchange leading to conversion of the CaP to biological apatite.¹²⁻¹⁴

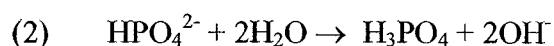
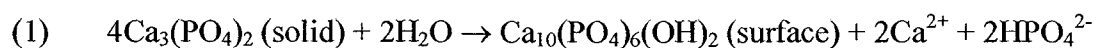
The chemical properties of CaP depend on both the temperature and the degree of hydration in either processing or the final environment. Solubility isotherms can predict the phase of CaP to be formed in a given set of conditions.^{15,16} Table 1 is a listing of biologically relevant CaP phases and their relative solubilities. There are two stable phases in the body environment: dicalcium phosphate dihydrate, DCPD, ($\text{CaHPO}_4 \cdot 2\text{H}_2\text{O}$) and hydroxylapatite, HA, ($\text{Ca}_{10}(\text{PO}_4)_6(\text{OH})_2$). Tricalcium ($\text{Ca}_3(\text{PO}_4)_2$) and tetracalcium ($\text{Ca}_4(\text{PO}_4)_2\text{O}$) phosphates (TCP and TTCP, respectively) are stable at higher tempera-

tures, but degrade when placed in an aqueous environment. Octacalcium phosphate (OCP) is metastable in the biological environment and has been proposed to occur as a precursor to HA in precipitation reactions.^{17,18}

TABLE 1. Listing of common calcium phosphates and relative CaP solubilities

Crystalline Phase	Stoichiometry	Molar Ca:P	Crystal structure	K_{sp}^{19}
Dicalcium phosphate dihydrate (DCPD, brushite)	$\text{CaHPO}_4 \cdot 2\text{H}_2\text{O}$	1.00	Monoclinic	2.39×10^{-7}
Dicalcium phosphate anhydrate (DCPA, monetite)	CaHPO_4	1.00	Triclinic	
Octacalcium phosphate (OCP)	$\text{Ca}_8\text{H}_2(\text{PO}_4)_6 \cdot 5\text{H}_2\text{O}$	1.33	Triclinic	1.05×10^{-47}
Tricalcium phosphate (TCP)	$\text{Ca}_3(\text{PO}_4)_2$	1.50	α - Monoclinic β - Rhombohedral	2.83×10^{-30}
Hydroxylapatite (HA)	$\text{Ca}_{10}(\text{PO}_4)_6(\text{OH})_2$	1.67	Hexagonal	3.37×10^{-58}
Tetracalcium phosphate (TTCP)	$\text{Ca}_4(\text{PO}_4)_2\text{O}$	2.00	Monoclinic	
Solubility of CaP phases, in increasing order $\text{HA} \ll \beta\text{-TCP} < \alpha\text{-TCP} < \text{TTCP} \ll \text{DCPD}^{1,13,19}$				

Several studies have demonstrated the conversion of DCPD, OCP, or TCP to HA by exposure to heat and/or aqueous solutions containing Ca and P as well as other ions.^{12,13,18,20-24} As mentioned previously, CaP can undergo dynamic changes with the biological environment to form HA, the most thermodynamically stable CaP. TCP converts to HA through the addition of water, as shown in equation (1).¹



The reaction in equation 1 causes an increase in the pH of the surrounding environment due to equation 2, which in turn increases the solubility of the TCP and enhances resorption,^{1,21,23} as well as further precipitation and ion exchange.¹²⁻¹⁴

Processing

Plasma Sprayed Calcium Phosphate Coating

Plasma spraying (PS) is the most widely used technique for applying CaP coatings; it is a line of sight, cost-effective process that is the industrial standard for applying many coatings.^{3,25-28} PS is a high temperature, low velocity technique having values around 2900°C and 150-180 m/s, respectively. The powder is thermally energetic when sprayed, followed by a mechanically energetic period when the molten ceramic impacts the target resulting in a minimum thickness of 30 to 40 μm .²⁹

The goal of coated biomedical implants is to optimize the dissolution of the ceramic coatings such that its strength and longevity enable bony ingrowth and, therefore, implant stability. In PS, CaP powder undergoes lattice distortion and forms coatings having residual stresses and secondary phases, predominantly α and β -TCP, with smaller amounts of amorphous CaP and calcium titanate.^{1,3,30-32} These changes contribute to porosity, low fatigue strength, and weak mechanical adherence of the coating to the metallic substrates.³² The residual stress, porosity, and the CaP phases produced in the PS coating are important factors that can influence coating dissolution rates, as seen in Table 2.^{1,33}

To decrease solubility, most PS coatings are subjected to a post deposition heat treatment which improves the crystallinity and homogeneity of phases present.³¹ Characterization of PS coatings becomes complicated by amorphous phases and can give inac-

TABLE 2. Summary of factors influencing dissolution rate of ceramic coatings

Increase dissolution rates	Decrease dissolution rates
Increase in surface area	Substitution of F ⁻ for OH ⁻ in HA
Decrease in crystallinity	Substitution of Mg ²⁺ for Ca ²⁺ in β -TCP
Decrease of crystal perfection	Greater presence of HA in coating
Decrease of crystal and grain size	

curate conclusions about phase identification.²⁸ During heat treatment between 630-1000°C, the grain size increases. At 800°C and above, HA transforms to α -TCP, β -TCP, tetracalcium monoxide diphosphate which leads to increased surface roughness.³⁴ Heat treatment conditions that maximize crystallinity and minimize secondary or less desirable phases of HA coatings do not occur at the same temperature.³⁵ This difference makes obtaining a PS CaP coating of both high crystallinity and phase purity difficult.

Alternate Coating Techniques

Other coating methods have been explored in an attempt to overcome the limitations of coating thickness, poor crystallinity, and multiple phases that result from plasma spraying. These include sputtering, pulsed laser deposition, immersion techniques, and electrodeposition. These thin-coating technologies may offer solutions to the problems incurred by PS CaP coatings.²⁹ High vacuum techniques, such as ion beam sputtering and RF magnetron sputtering, can also be used to produce CaP coatings but may still require post-deposition heat treatment to obtain a more homogeneous and stable CaP phase such as HA.³⁶⁻³⁹ Pulsed laser deposition is an evaporative process capable of depositing CaP coatings with variable surface roughness. As-deposited CaP coatings obtained by pulsed laser deposition contain amorphous phases and require post treatment to improve crystallinity.⁴⁰ Immersion techniques have been shown to yield a bioactive CaP layer that does

not obstruct pores in porous titanium surfaces.^{41,42} However, time-consuming CaP deposition can result from extended induction times for precipitation.⁴³

Electrodeposition of CaP from solution on titanium substrates offers an alternative method of thin coating preparation for biomedical implants. Unlike line-of-sight techniques, such as plasma spraying or sputtering, CaP deposition from aqueous solutions allows uniform coating of complex implant geometries.⁴⁴ Electrodeposition can be divided into two deposition techniques: electrophoretic deposition and electrolytic deposition.

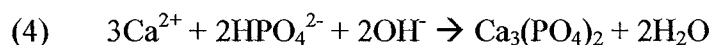
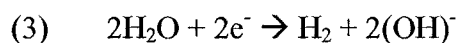
Electrophoretic Deposition

Electrophoretic deposition is achieved via motion of charged particles towards an electrode under applied electric field. Submicron HA powder is prepared via chemical precipitation and added to an electrochemical bath. It has been found that water interferes with electrophoretic transport, and, therefore, electrophoretic deposition of non-calcined HA powders.^{45,46} Due to this, most electrophoretic deposition studies have found success in nonaqueous media.⁴⁵⁻⁴⁸ This type of deposition limits itself in that it is highly dependent upon materials and process variables such as particle size and agitation of the bath.

Electrolytic Deposition

Unlike electrophoretic deposition, electrolytic deposition (ELD) drives ions out of solution to form coatings. Metal ions or complexes are hydrolyzed by an electro-generated base in ELD to form oxide or hydroxide films on the cathodic substrate.⁴⁶ Specifically for CaP deposition in aqueous solutions, water molecules are reduced to form H₂

gas and OH^- at the cathode, enabling reaction with the Ca^{2+} and HPO_4^- ions in the electrolyte as illustrated in the following possible reactions.⁴⁹⁻⁵¹



Shirkhanzadeh has had much success with using this method to deposit ceramic coatings on conductive substrates.^{49,52-54} It has been illustrated that by using a simple electrolytic bath, it is possible to deposit single phase CaP coatings, yet some post treatment was required to convert to HA.^{53,54}

Substrate Modification

Surface modifications have been performed on titanium substrates to alter the native oxide layer, TiO_2 (rutile). Implant surfaces have been pretreated with self-assembled monolayers containing carboxylate or phosphate head groups to reduce the induction times for CaP precipitation in immersion techniques.⁵⁵ These head groups were shown to accelerate the induction of CaP deposition.⁵⁶ This can become an expensive and/or complicated intermediate step. Alternately, it has been found that exposing titanium to different environments, including combinations of nitric and phosphoric acids and steam, affected the tenacious oxide layer inherent to the material. Surface changes included roughness as well as presence of phosphate and carbon in the oxide.⁵⁷⁻⁵⁹

Coating Performance

Coating Adhesion

There is a need for improved bonding between the metallic substrates and PS CaP coatings for long term stability; coatings need to transfer load from the bone to the underlying metal substrate. The stability of the implant is influenced by the nature of the surface and the phases present.³¹ As bony ingrowth occurs, the bond strength of the coating with the bone exceeds that with the substrate. The CaP coated implants then fail at the substrate/coating interface; this interface needs to be protected due to its weakness in shear loading.^{60,61}

Other coating techniques have been investigated in an attempt to improve on bond strengths for plasma sprayed coatings. Zeng found pulsed laser deposited CaP coating to have bond strengths of 31.1 ± 13.1 MPa on titanium polished to 600 grit.⁴⁰ Using ion beam sputter deposition, Rigney reported strengths ranging from 8.67 to 47.28 MPa.³⁹ Kumar et al. reported values of less than 0.7 MPa for ELD brushite coatings, citing failure within the ceramic.⁶² Han reported values as high as 14 MPa for an electrodeposited CaP coating.⁶³ While some of the techniques are comparable to the reported values for plasma spraying, 30.25 ± 1.72 MPa,⁶⁴ none are decisively stronger.

Cell Adhesion

In vivo processes occur at microscopic and chemical levels where differences in the crystallinity, chemistry, and morphology of the coating structure are important. Apatite has been discovered to form on pure gel-silica soaked in simulated body fluid.^{65,66} One study found that a silica hydrogel on the surface induced apatite formation in simu-

lated body fluid. After nuclei formed, they grew in a spherulitic form by consuming Ca^{2+} and PO_4^{3-} ions from the fluid. Results indicated silanol groups on surface accelerated apatite nucleation.⁶⁶ Apatite has also formed on titanium in simulated body fluid. It is assumed that $\text{Ti}(\text{OH})_4$ groups on the surface attract calcium and phosphate from the body fluid and form apatite in parallel with the wound healing process.⁶⁷

A goal for implant success is to optimize the dissolution of ceramic coatings such that the strength and longevity of the coating benefit bony ingrowth and implant stability. Improved bonding with bone is an important factor for non-cemented orthopaedic and dental implant performance. While this has been achieved with coated implants, the exact mechanisms that control the bonding are still under investigation. It is felt by some that cell adhesion may be a key step in understanding the bone adhesive properties of biomedical implants.⁶⁸⁻⁷¹ Cell adhesive proteins, such as fibronectin and vitronectin, are present in blood which coats implants upon insertion into bone. Integrins contribute to binding cells to extracellular proteins like fibronectin and vitronectin. In a study by Kilpadi et al., it was found that bulk HA had greater adhesion of fibronectin and vitronectin, purified integrins, and osteoblast precursor cells than titanium and 316L stainless steel.⁷² This adhesion may provide an explanation for the interfacial bond and direct apposition of CaP with bone.

Proposed Study

Electrochemical deposition provides a low temperature method of applying calcium phosphate with controlled crystal structure on titanium substrates. In multiple publications,⁴⁹⁻⁵⁴ it has been shown that calcium phosphate can be directly deposited on the surface from an electrolytic solution, but there has been little investigation of the ELD

coating bond strength. From solubility curves, it is found that DCPD/DCPA is the stable CaP phase in more acidic solutions, while HA is stable in neutral to basic solutions.¹⁸ Combining this information with the control available with the ELD process, this research has been designed to explore the feasibility of electrolytically depositing biologically active CaP on titanium substrates. Based on the literature, exposing the titanium in a solution of phosphoric acid will modify the surface of the substrates. It is hypothesized that the modified surface will provide attachment sites in the form of phosphate groups that will enable the formation of a stronger bond between the substrate surface and the deposited ceramic coating, improving the bond strength of the applied coating.

The objective of this study was to develop a method to apply a biocompatible CaP coating of desired solubility and integrity on acid etched titanium with a strong bond to the substrate.

Specific Aims

1. Electrodeposit a resorbable calcium phosphate coating on modified titanium substrates using constant current techniques and an unbuffered electrolyte.
 - a. Fabricate a CaP coating on Ti substrates with either NPAS or PMOD treatment.
 - b. Ascertain crystal structure and coverage.
 - c. Measure bond strength.
 - d. Quantify the amounts of elements released from coating in a biological saline.

2. Electrodeposit a nonresorbable coating on modified titanium substrates in an unbuffered CaP electrolyte.
 - a. Fabricate a hydroxylapatite coating on Ti substrates with either NPAS or PMOD treatment.
 - b. Ascertain crystal structure and coverage.
 - c. Measure bond strength.
3. Determine biocompatibility of ELD HA coated samples compared to uncoated Ti substrates and sintered HA pellets.
 - a. Quantitatively compare the elements released by ELD HA and Ti to those released by sintered HA pellets in a biological saline.
 - b. Characterize the properties of the surfaces post exposure to biological saline solution.
 - c. Compare the cell morphology of osteoprogenitor cells on the different surfaces.
4. Demonstrate control of the electrolytic deposition system to deposit desired CaP coating.
 - a. Develop an understanding of the electrolytic deposition of CaP using an unbuffered CaP containing electrolyte.
 - b. Determine effects of adjusting pH, ion concentration, and applied current density on CaP deposition.
 - c. Utilize thermodynamics, kinetics, and deposition parameters to optimize interface chemistry for desired CaP deposition.

ELECTROLYTIC DEPOSITION OF A RESORBABLE CALCIUM PHOSPHATE
COATING

by

REBECCA SHUMATE O'CONNOR DAVIS, RAMAKRISHNA VENUGOPALAN,
AND GREGG M. JANOWSKI

In preparation for *Journal of Biomedical Materials Research Part B: Applied
Biomaterials*

Format adapted for dissertation

ABSTRACT

The purpose of this study was to deposit a resorbable calcium phosphate (CaP) using electrolytic deposition (ELD) on commercially pure titanium (cpTi) substrates, either passivated with nitric acid (NPAS) or treated further and pickled with phosphoric acid (PMOD) prior to ELD. The ELD process was optimized to deposit a continuous CaP coating that consisted of mostly octacalcium phosphate (OCP) and hydroxylapatite (HA). The coatings were deposited at 37°C and examined using SEM, EDS, XRD, XPS, FTIR, and coating bond strength testing. Solubility of the coatings was investigated over a 14 day incubation period at 37°C in Earle's Balanced Salt Solution (EBSS) and ion content was measured using ICP. The CaP was determined to be resorbable in that it released Ca and P into the EBSS over the 14 day period. The cpTi surface treatments had no detectable effect on the final ELD CaP coating. ELD CaP had high bond strength to the cpTi, approaching values above the rating limits for the system (PMOD = 80.11 ± 5.87 MPa, $n = 6$ and NPAS = 69.43 ± 12.17 MPa, $n = 8$). ELD is an easily controllable system capable of consistently depositing continuous, resorbable CaP at low temperatures.

INTRODUCTION

Calcium phosphates (CaP) have been used in orthopedic and dental devices for over 20 years. When used as a coating, CaP provides an osteoconductive surface that pairs with the mechanical strength of the underlying metal to give an implant that provides improved functionality.¹⁻⁵ The coating protects the biological environment from metal ion release of the substrate and has been shown to form a direct bond with bone.^{6,7}

The CaP coating's chemical bond and subsequent direct apposition with bone allows transfer of the load to the metal substrate.

The most relevant CaP phases in the biological environment include hydroxylapatite (HA, $\text{Ca}_{10}(\text{PO}_4)_6(\text{OH})_2$), octacalcium phosphate (OCP, $\text{Ca}_8\text{H}_2(\text{PO}_4)_6 \cdot 5\text{H}_2\text{O}$), dicalcium phosphate anhydrous (monetite, DCPA, CaHPO_4), dicalcium phosphate dihydrate (brushite, DCPD, $\text{CaHPO}_4 \cdot 2\text{H}_2\text{O}$), tricalcium phosphate (α - and β -TCP, $\text{Ca}_3(\text{PO}_4)_2$), and tetracalcium phosphate (TTCP, $\text{Ca}_4\text{P}_2\text{O}_9$). Each of these phases has a different crystal structure, morphology, molar ratio, degree of hydration, and solubility, which give rise to differing behavior in the biological environment.^{8,9} The solubility of the CaP relative to the biological environment leads to the classification as either being resorbable or nonresorbable.

CaP and the biological environment form a dynamic system with the coating acting as a source, or sink, for ions, which in turn can change the phases. Some CaP phases are resorbed and/or completely transformed while in the body due to the pH and ions present in the biological environment.⁹⁻¹¹ The CaP solubility isotherms show that DCPA and DCPD are the stable phases in more acidic environments ($\text{pH} < 4$). OCP is stable at higher temperatures in neutral pH but at lower temperatures will form HA, the most thermodynamically stable phase over neutral to basic pH values.^{12,13} DCPA, DCPD, and OCP are metastable phases in the biological environment and are known precursors that can convert through hydration and ion exchange to form HA. Physicochemical dissolution, ion substitution, and precipitation reactions take place simultaneously between the CaP and surrounding environment driven by factors such as an increased pH, availability of ions (Ca^{2+} , PO_4^{3-} , OH^- , etc.), and temperature.^{8-12,14-16}

Most commercially available CaP coatings are applied by plasma spraying.

Plasma spraying is a high temperature, high energy process that melts the ceramic powder and impacts it on the metal substrate where it cools on contact, forming a mechanical bond with the substrate. The high temperature and rapid cooling result in areas of amorphous coating, which are highly soluble. Additionally, the large thermal mismatch of the ceramic and the metal causes internal stresses in the coating that can result in spallation. Plasma sprayed coatings are typically subjected to a post-heat treatment to minimize both of these effects.^{6,17-19}

Electrolytic deposition (ELD) is a promising technique that can overcome these thermal issues of plasma sprayed coatings. ELD uses the simple chemical process of hydrolysis of metal ions, or complexes, to deposit CaP on metallic substrates at low temperatures by driving ions out of solution. It is a non-line-of-sight process and lends itself well to the complex geometries of orthopedic and dental implants. There has been success in depositing CaP on titanium using ELD at temperatures well below those used for plasma spraying.^{16,20-23} The ELD coating composition and thickness can be controlled by adjusting the deposition time, applied current, temperature, and/or bath chemistry.

The focus of this study was to fabricate a resorbable CaP coating on titanium substrates by applying the basic principles of the CaP solubility isotherms to ELD. These titanium substrates were treated with different acids to investigate the effects of surface chemistry on the resulting coating in terms of morphology, crystallinity, phase composition, bond strength, and solubility.

MATERIALS AND METHODS

Fabrication

Unalloyed titanium disks, commercial purity, grade 2, ($\varnothing = 16$ mm) were wet ground through 600 grit SiC paper. The disks were then cleaned and passivated per ASTM F86 guidelines by sonicating in acetone, distilled water, ethanol, and distilled water, and soaking in 30% nitric acid for 20 minutes. Half of the substrates were treated further by immersion in 30% phosphoric acid for 20 minutes (PMOD). Those not treated in phosphoric acid will be referred to as NPAS.

A bath with 6.10×10^{-4} M concentration of Ca^{2+} and 6.10×10^{-4} M concentration of PO_4^{3-} was formulated to deposit the acidic phosphate phases, dicalcium phosphate anhydrous (monetite, DCPA) and dicalcium phosphate dihydrate (brushite, DCPD), based upon solubility isotherms of CaP. The bath was composed of NaCl, CaCl_2 , and KH_2PO_4 (reagent grade), with an ionic strength of 0.15 M. The starting bath pH was adjusted to 4.0 ± 0.1 using HCl. A new bath was used for each coating deposition.

All experiments were performed in double-walled glass vessels at 37°C and purged with humidified nitrogen to remove oxygen and deter CaCO_3 formation. A Hewlett Packard 6633A System DC power supply was connected to the titanium substrate (cathode) and a Pt/Nb wire mesh (anode). Figure 1 is a schematic of the deposition system. A constant current density was maintained for 2 h. Bath temperature and pH were measured before and after deposition to monitor consistency. The coated substrates were then rinsed with distilled water and ethanol, dried with a heat gun on low setting, and stored in a desiccator until further analysis.

Depositions were performed on NPAS and PMOD substrates for the preliminary studies at the following current densities: 100, 150, 200, 250, and 300 mA/cm². A current density of 150 mA/cm² was the optimum deposition current density based on coating uniformity and continuity and was used for the remaining experiments. Mass was recorded before and after coating deposition to estimate coating thickness.

Characterization

X-ray Diffraction

A Siemens D500 diffractometer was used to identify the calcium phosphate phase in the coating. The scans used a 0.02 ° 2 θ step size for 6 s/step over a 15-90° 2 θ range and a CuK α radiation source (40 keV, 25 mA). The scans were compared with International Centre for Diffraction Data (ICDD) files.

Scanning Electron Microscopy/ Electron Dispersive Spectroscopy

SEM was used to examine morphology of the substrates and coated disks (both NPAS and PMOD) using a Phillips 515 SEM with an accelerating voltage of 30 keV. The coated samples were cleaned in methanol before sputter coating with gold for analysis. EDS was also performed using a 500X scan area, standardless quantification methods, and used 15 keV to quantify the Ca to P molar ratio.

X-ray Photoelectron Spectroscopy

X-ray photoelectron spectroscopy was performed at the Surface Analysis Laboratory at the University of Alabama with a Kratos AXIS 165 Multitechnique Electron Spec-

trometer using a monochromatic Al (1487 eV) x-ray source that penetrated less than 5 nm into the surface. High-resolution scans were performed at 40 eV for 3 samples of each of the following groups: uncoated NPAS, uncoated PMOD, coated NPAS, and coated PMOD. Curve fitting of spectra was performed using Spectral Data Processor v3.0.

Fourier Transform Infrared Spectroscopy

Fourier Transform Infrared Spectroscopy (FTIR) was performed at the Center for Advanced Materials at Tuskegee University. Samples were examined using a Nicolet Nexus 470 FT-IR operated in reflectance mode. The spectra were collected using 64 scans from 4000 to 400 cm^{-1} with 4 cm^{-1} resolution.

Bond strength

Epoxy coated studs were affixed to the coatings, and the normal stress required to detach the stud from the sample surface was measured. Studs were affixed with a clamp and cured for 1 h at 150°C to ensure mounting perpendicular to the surface. After cooling, the samples were tested using the Sebastian Five Strength Tester (Quad Group). Samples were loaded at a rate of 5 kg/s. After testing, samples and studs were visually inspected using stereomicroscopy as well as SEM/EDS and XPS to determine area of failure.

Solubility

CaP coated NPAS and PMOD disks were covered with 1 mL of Earle's Balanced Salt Solution (EBSS, part number E3024, Sigma) and placed in an incubator at 37°C with

5% CO₂ flow. Ion content was measured at 1 h, 24 h, and at days 2, 3, 5, 7, 10, and 14, using Inductively Coupled Plasma-Optical Emission Spectroscopy (ICP, CV3300, Perkin Elmer). The solution was replaced at each time period with fresh EBSS. Wells without samples were filled with EBSS and used as controls to adjust for possible evaporation.

RESULTS AND DISCUSSION

Substrate Treatment

The titanium disks were characterized after the different acid surface treatments using SEM, EDS, XRD, and XPS. The acid treatments did alter the surface of the NPAS and PMOD titanium substrates. As was expected, phosphorous was detected by XPS on the uncoated PMOD substrates, and none was found on the uncoated NPAS. There were no other measurable differences found using the other characterization techniques. SEM revealed no comparable differences in surface morphologies while only titanium and nitrogen were detected for both NPAS and PMOD treatments by EDS. The spectra collected using XRD were identical for both surface treatments.

Coating Process

The coatings fabricated in preliminary studies were visually inspected using a stereoscope to determine the current density that yielded the best coating coverage. Based on these inspections, 150 mA/cm² was found to be the optimum current density for deposition of the CaP coating; CaP deposited at 150 mA/cm² appeared continuous. Coatings deposited on both NPAS and PMOD substrates below this current density had discontinuous coverage, while those formed at higher currents showed evidence of localized

spalling due to the increased H_2 gas evolution. Figure 2 shows typical CaP coatings from the different current densities.

Coated samples were sonicated in methanol for approximately 2 min to investigate the early stages of the coating process. Figure 3 illustrates that this process eradicated most of the coating, but made the nucleation sites on the substrate surface visible. There was good adhesion since coating was still present on the substrate surface after sonication for both treatments. More nucleation sites were found on the PMOD surface than the NPAS substrate.

Preliminary samples coated at 100 mA/cm^2 were then examined without sonication. It was found on these preliminary samples with discontinuous coatings that there was more coating present, as well as greater definition of crystal structure on the CaP coated PMOD substrate than the CaP coated NPAS substrate. These findings are consistent with the nucleation site observations on the sonicated samples. Such distinctions were not as evident on the continuous coatings deposited at 150 mA/cm^2 , as seen in Figure 4. The coatings deposited at 150 mA/cm^2 had very similar crystal definition and continuity for both substrate treatments.

Samples mounted in cross section revealed a continuous ridge of dense coating ($10\text{-}15 \text{ }\mu\text{m}$) with areas of small and large grains up to $10 \text{ }\mu\text{m}$ in size growing upward from the substrate. Representative images of the coatings in cross section are shown in Figure 5.

The change in sample mass during deposition was used to calculate the coating thickness. Coating thickness was estimated to be $13 \text{ }\mu\text{m}$ on all of the coated substrates

deposited at 150 mA/cm^2 for 2 h. This value corresponds with the coating thickness observed in Figure 5.

Coating Characterization

XRD was performed on the CaP coatings to determine the phase(s) present in the deposited coatings and what effects the underlying surface treatments had on the phases. The ELD CaP coated NPAS and PMOD substrates had similar XRD spectra. Figure 6 is a representative scan of PMOD and NPAS coated disks; the two scans were indistinguishable. The scans were compared with ICDD files (Figure 7). There was a notable shift between ICDD files and the collected spectra. This was especially evident for Ti, which had the greatest intensity for the (100) peak. The CaP coating best matched OCP (ICDD 26-1056) and HA (ICDD 9-432), with Ti peaks (ICDD 5-682) detected. There was little or no correlation with the ICDD file for DCPD (9-77) for coatings on either substrate treatment, missing the four highest peaks from the card file.

CaP coated NPAS and PMOD substrates were analyzed using EDS to determine the molar ratio of calcium to phosphorous. Data obtained from the coating surfaces indicate values that support the combined presence of OCP (Ca:P = 1.33) and HA (Ca:P = 1.67): ELD CaP coated NPAS = 1.46 ± 0.017 , and ELD CaP coated PMOD = 1.46 ± 0.027 , not a statistically significant difference. A higher Ca:P ratio was noted on the CaP coating surface using XPS: CaP coated NPAS = 1.85 ± 0.06 , and CaP coated PMOD = 1.72 ± 0.12 , not a statistically significant difference.

Survey scans using XPS indicated the presence of carbon on the surfaces of all of the disks. Analysis of a high-resolution scan of a CaP coated substrate showed it to be

predominantly in the form of adventitious carbon with some carbonate presence. No titanium was detected on the high-resolution scans of the coated samples, again supporting the presence of a continuous coating, as was indicated previously with microscopy.

FTIR was performed on the coatings to determine the CaP phases present. The as-collected spectra did not give a clear determination of HA or OCP. The spectra were corrected adapting a procedure outlined by Gadaleta et al. by adjusting the baseline between 800 and 1300 cm^{-1} and taking the second derivative to identify peaks.²⁴ This was performed using the automatic presets in OMNIC 6.0a software by Thermo Nicolet. There were many of the vibration peaks for PO_4^{3-} visible which were compared to those given in publications.^{14,24,25} However, there were no defining PO_4^{3-} peaks that could distinguish the spectra as any particular CaP phase. Peaks associated with OH^- were not seen; hydroxyl groups are present in both OCP and HA. The absence of peaks in the spectra for ELD coating is most likely a result of the testing technique. The spectra were obtained in reflectance mode, where the as-deposited coatings were placed directly on the KBr window. The roughness of the sample surface can affect the spectra and hide certain peaks. Commercially available HA (Fisher) was pressed into pellet form, and sintered and scanned on FTIR following procedure used for the ELD CaP coatings. Again, no OH^- peak was detected, supporting the aforementioned surface roughness effect.

Bath temperature was maintained at 37°C for the duration of the deposition, but pH changed from 4.0 ± 0.1 at the start to 7.7 ± 0.1 after deposition. The starting bath was formulated to deposit DCPD and was under saturated for OCP and HA. DCPD becomes unstable at higher pH with respect to both OCP and HA. As the CaP coating was deposited, the higher pH would convert the DCPD through the hydrolysis reactions at the cath-

ode and/or deposit other phases of CaP stable at higher pH values, including OCP and HA.

Bond Strength Testing

Bond strengths of all coatings were tested, including those from the preliminary studies and are included in the graph in Figure 8. The epoxy is reported by Quad Group to have strength of ~ 69 MPa, which is the upper limit of this bond strength quantification. Uncoated substrates were measured as a baseline comparison. The average bond strengths for the uncoated substrates were 86.25 ± 4.39 MPa, $n = 8$ for NPAS and 83.03 ± 7.80 MPa, $n = 8$ for PMOD. All averages from CaP coated disks were near or above the rated epoxy strength. The mean strength for CaP coated PMOD substrates was higher than that for NPAS deposited at 150 mA/cm^2 (80.11 ± 5.87 MPa, $n = 6$ and 69.43 ± 12.17 MPa, $n = 8$, respectively), but the difference was not statistically significant (t-test, $p > 0.05$). Failure occurred between the coating and substrate or the epoxy and the stud for the coated samples. Figure 9 is representative of the surface and corresponding stud after the adhesion test. There was no evidence of failure within the coating; XPS of the failure areas only detected titanium or epoxy.

Due to the high bond strength values of the CaP coatings, thicker coatings were deposited using doubled time, doubled initial calcium and phosphorous concentrations, and maintaining all other starting deposition conditions. The bond strength values greatly decreased for both NPAS and PMOD (17.09 ± 6.96 MPa, $n = 3$ and 16.48 ± 3.61 MPa, $n = 2$ respectively). Figure 10 compares the adhesion values for coatings deposited at 150 mA . The coatings deposited for 4 h were difficult to handle and were susceptible to

spalling. Failures of the 4-hour deposition specimens were consistently within the coatings. Table 1 compares the bond strengths measured for different CaP coating depositions on titanium substrates using similar testing methods. Published values were all lower than those obtained in this study.^{16,26-28}

TABLE 1. Comparison of coating adhesion values

Coating Method	Bond Strength (MPa)
ELD CaP 150 mA/cm ²	NPAS 69.43 ± 12.17 PMOD 80.11 ± 5.87
Electrodeposition ¹⁶	< 0.7
Ion Beam Sputter Deposition ²⁶	47.28 - 8.67
Pulsed Laser Deposition ²⁷	600 grit 31.1 ± 13.1 Polished 12.1 ± 5.3
Electrodeposition ²⁸	14
Plasma Spray ²⁸	~ 30

Solubility in Earl's Balanced Salt Solution

Coated disks were immersed in EBSS to determine whether the CaP coatings were soluble as a predicative indicator of behavior in a biological environment. ELD coatings released calcium and phosphorous into solution over the 14 day period. Coated NPAS and PMOD dissolution rates were indistinguishable. Figure 11 illustrates the cumulative release of calcium and phosphorous into the solute as compared to control EBSS. This result was supported by loss of coating continuity observed over the time period. Areas of coating loss were characterized by grains with pronounced needle-like shells, shown in Figure 12, replacing the as-deposited structure in Figure 4. The release of Ca and P ions in the process of physicochemical dissolution and reprecipitation have been related to the early stages involved in the steps leading to CaP adhesion with bone.¹⁰

The change in the CaP coating was reflected in EDS values after the 14 day period. The Ca:P decreased for both surface treatments: NPAS CaP = 1.23 ± 0.22 and PMOD CaP = 1.27 ± 0.15 . There was no statistical difference between the two treatments for the EDS values. XRD of these surfaces in Figure 13 revealed that surface treatment still had no effect on the coating and echoed the loss of crystallinity observed in the images.

CONCLUSIONS

1. CaP coatings were deposited on NPAS and PMOD titanium substrates using ELD.
2. Coatings were consistently CaP predominantly composed of OCP and HA on both substrates using XRD. This was supported by EDS and XPS.
3. System was easily optimized for coating deposition by adjusting parameters.
4. Differences between substrate treatments were minimal at the current level of characterization. Phosphorous was detected on the surfaces of uncoated PMOD substrates using XPS, yet there were no discernable differences in the final coatings.
5. Bond strength studies found that the bond strengths of the CaP coatings were high, but due to the measured values being so great, the values cannot be used to truly quantify the adhesion of the coating to the substrate.
6. More nucleation sites in the early stages of deposition on the CaP coated PMOD compared to the CaP coated NPAS did not translate to a measurable difference in coating bond strengths.

7. Solubility studies revealed that the ELD CaP coatings were resorbed in EBSS. Both calcium and phosphorous were released into solution over the 14 day period resulting in visible changes to the CaP coating.

ACKNOWLEDGEMENTS

The authors would like to thank Dr. Earl T. Ada for his assistance with training and analysis on the XPS in the Surface Analysis Laboratory at the University of Alabama, Tuscaloosa, AL. Additionally, we would like to acknowledge Mr. Ed Calvert of Wallace State Community College, Hanceville, AL for allowing generous access to the ICP at their facility and Dr. Derrick Dean for providing FTIR data.

REFERENCES

1. Morris HF, Ochi S. Hydroxyapatite-coated implants: a case for their use. *Journal of Oral and Maxillofacial Surgery* 1998;56(11):1303-1311.
2. Jarcho M. Calcium phosphate ceramics as hard tissue prosthetics. *Clinical Orthopaedics and Related Research* 1981;157:257-278.
3. Cook SD, Thomas KA, Dalton JF, Volkman TK, Whitecloud TS, Kay JF. Hydroxylapatite coatings of porous implants improves bone ingrowth and interface attachment strength. *Journal of Biomedical Materials Research* 1992;26:989-1001.
4. Cook SD, Thomas KA, Kay JF, Jarcho M. Hydroxyapatite-coated porous titanium for use as an orthopedic biologic attachment system. *Clinical Orthopaedics and Related Research* 1988;230:303-312.
5. Suchanek W, Yoshimura M. Processing and properties of hydroxyapatite-based biomaterials for use as hard tissue replacement implants. *Journal of Materials Research* 1998;13(1):94-117.

6. Ducheyne P, Healy KE. The effect of plasma-sprayed calcium phosphate ceramic coatings on the metal ion release from porous titanium and cobalt-chromium alloys. *Journal of Biomedical Materials Research* 1988;22(12):1137-1163.
7. Dalton JE, Cook SD. *In vivo* mechanical and histological characteristics of HA-coated implants vary with coating vendor. *Journal of Biomedical Materials Research* 1995;29:239-245.
8. Bioceramics of calcium phosphate. Boca Raton: CRC Press; 1983.
9. LeGeros RZ. Calcium phosphates in oral biology and medicine. San Francisco: Karger; 1991.
10. Ducheyne P, Radin S, King L. The effect of calcium phosphate ceramic composition and structure on *in vitro* behavior. I. Dissolution. *Journal of Biomedical Materials Research* 1993;27:25-34.
11. Daculsi G, LeGeros RZ, Nery E, Lynch K, Kerebel B. Transformation of biphasic calcium phosphate ceramics *in vivo*: ultrastructural and physicochemical characterization. *Journal of Biomedical Materials Research* 1989;23(8):883-894.
12. Brown WE, Chow LC, inventors; American Dental Association Health Foundation, assignee. Dental restorative cement pastes. United States patent 4518430. 1985 May 21.
13. Johnsson MS, Nancollas GH. The role of brushite and octacalcium phosphate in apatite formation. *Critical Reviews in Oral Biology and Medicine* 1992;3(1-2):61-82.
14. Kumar M, Xie J, Chittur K, Riley C. Transformation of modified brushite to hydroxyapatite in aqueous solution: effects of potassium substitution. *Biomaterials* 1999;20(15):1389-1399.
15. Fulmer MT, Ison IC, Hankermayer CR, Constantz BR, Ross J. Measurements of the solubilities and dissolution rates of several hydroxyapatites. *Biomaterials* 2002;23:751-755.

16. Kumar M, Dasarathy H, Riley C. Electrodeposition of brushite coatings and their transformation to hydroxyapatite in aqueous solutions. *Journal of Biomedical Materials Research* 1999;45(4):302-310.
17. Radin SR, Ducheyne P. Plasma spraying induced changes of calcium phosphate ceramic characteristics and the effect on *in vitro* stability. *Journal of Materials Science: Materials in Medicine* 1992;3:33-42.
18. Ji H, Marquis PM. Effect of heat treatment on the microstructure of plasma-sprayed hydroxyapatite coating. *Biomaterials* 1993;14(1):64-68.
19. Yang YC, Chang E. Influence of residual stress on bonding strength and fracture of plasma-sprayed hydroxyapatite coatings on Ti-6Al-4V substrate. *Biomaterials* 2001;22(13):1827-1836.
20. Ban S, Maruno S. Deposition of calcium phosphate on titanium by electrochemical process in simulated body fluid. *Japanese Journal of Applied Physics, Part II: Letters* 1993;32:1577-1580.
21. Ban S, Maruno S. Morphology and microstructure of electrochemically deposited calcium phosphates in a modified simulated body fluid. *Biomaterials* 1998;19(14):1245-1253.
22. Shirkhanzadeh M, inventor; Queen's University at Kingston, assignee. Method for depositing bioactive coatings on conductive substrates. United States patent 5205921. 1993 April 27.
23. Shirkhanzadeh M. Direct formation of nanophase hydroxyapatite on cathodically polarized electrodes. *Journal of Materials Science: Materials in Medicine* 1998;9:67-72.
24. Gadaleta SJ, Paschalis EP, Betts F, Mendelsohn R, Boskey AL. Fourier transform infrared spectroscopy of the solution-mediated conversion of amorphous calcium phosphate to hydroxyapatite: New correlations between x-ray diffraction and infrared data. *Calcified Tissue International* 1996;58:9-16.
25. Leeuwenburgh S, Wolke J, Schoonman J, Jansen J. Electrostatic spray deposition (ESD) of calcium phosphate coatings. *Journal of Biomedical Materials Research* 2003;66A:330-334.

26. Rigney E. Characterization of ion-beam sputter deposited Ca-P films [Dissertation]. Birmingham, AL: University of Alabama at Birmingham; 1989.
27. Zeng H. Evaluation of bioceramic coatings produced by pulsed laser deposition and ion beam sputtering [Dissertation]. Birmingham, AL: University of Alabama at Birmingham; 1997.
28. Han Y, Fu T, Lu J, Xu K. Characterization and stability of hydroxyapatite coatings prepared by an electrodeposition and alkaline-treatment process. *Journal of Biomedical Materials Research* 2001;54(1):96-101.

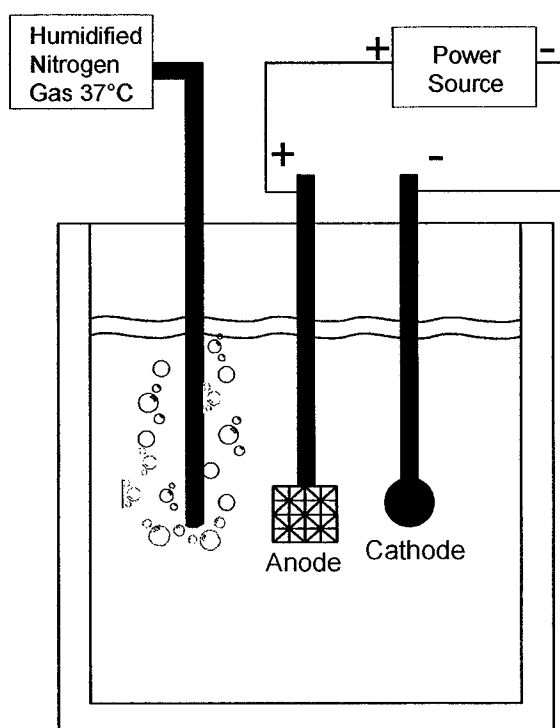


Figure 1. Electrochemical deposition cell showing major components.

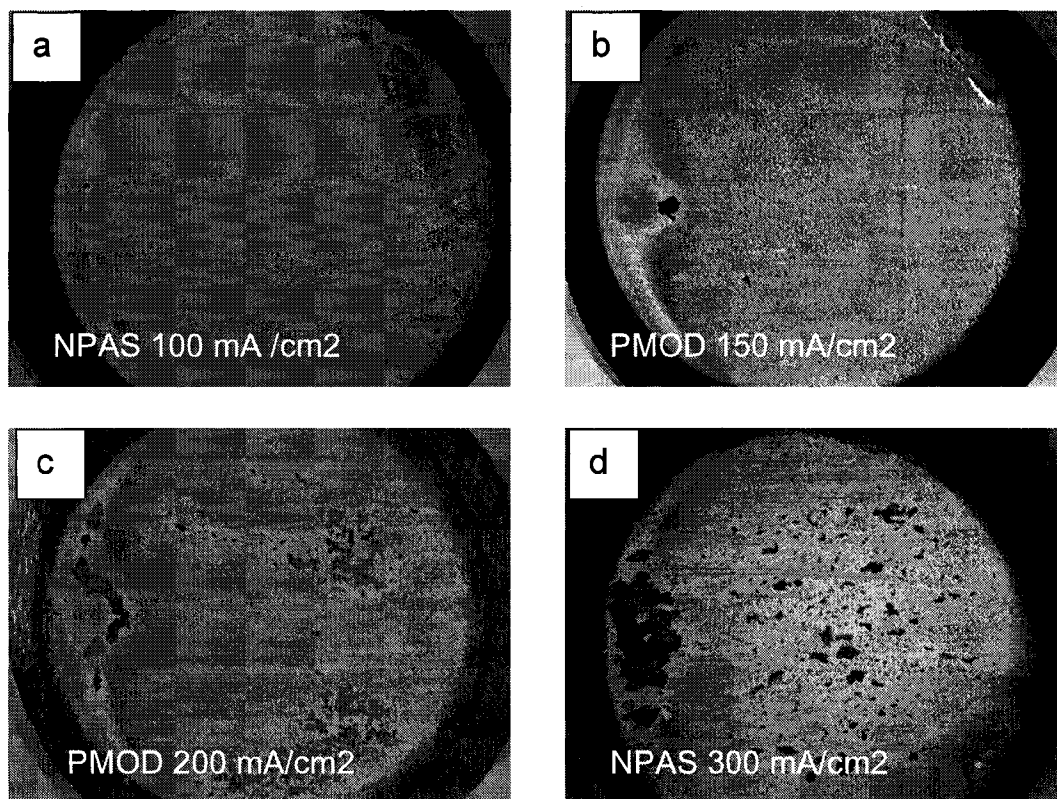


Figure 2. Representative photomicrographs of coatings deposited at various current densities. Below the optimum current density of 150 mA/cm^2 coatings were discontinuous (a), while those deposited at higher current densities were subject to spalling (c) and (d).

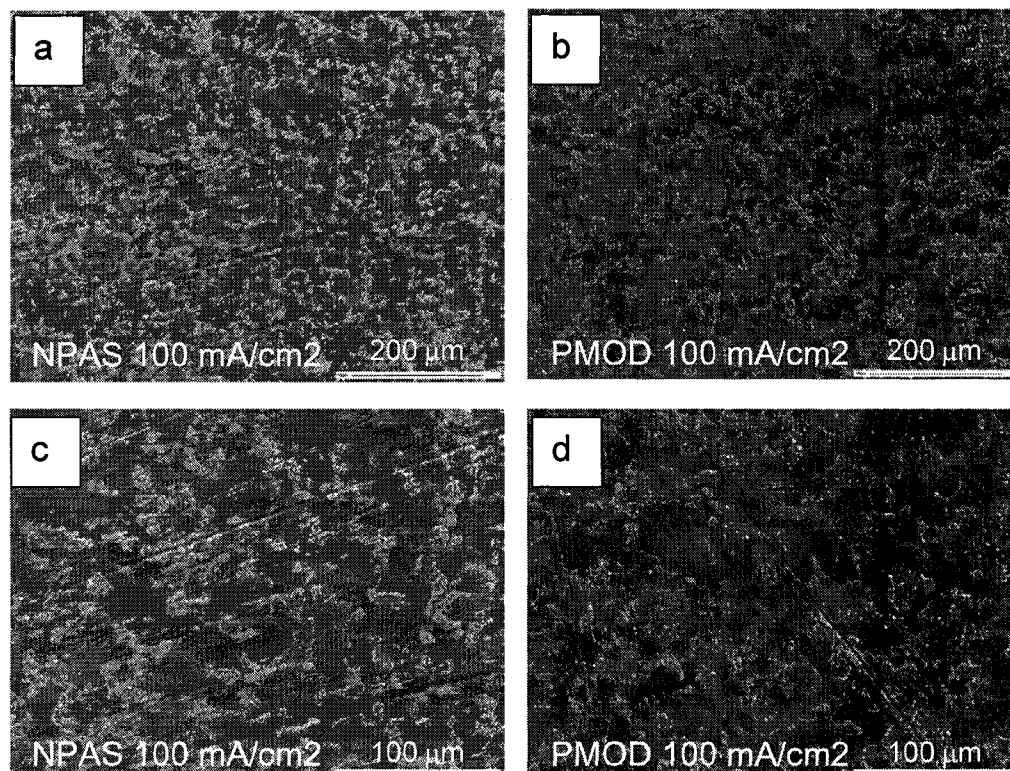


Figure 3. SEM micrographs of coated substrates after sonication in methanol. More nucleation sites remain on the PMOD surface (b) and (d) than on the NPAS surface (a) and (c).

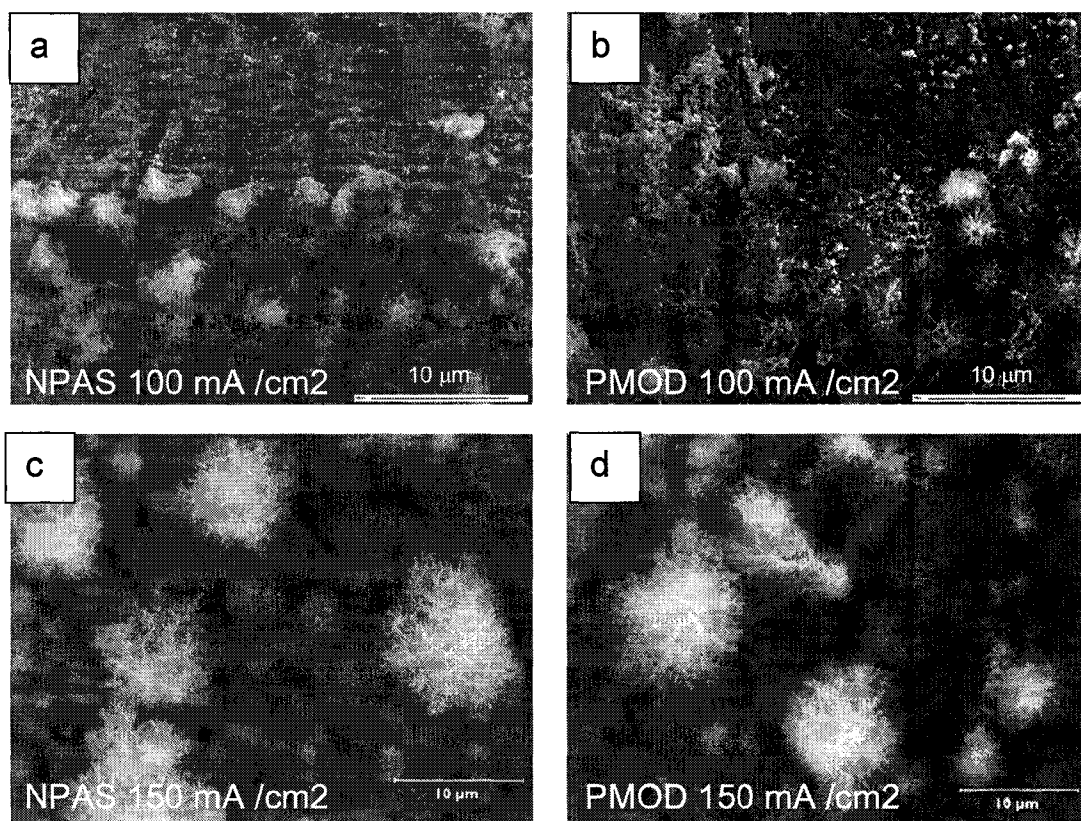


Figure 4. Micrographs of as deposited coatings deposited at either 100 or 150 mA/cm². PMOD coatings exhibited better crystal definition at lower current density (b), but the distinction was lost at higher deposition currents (d).

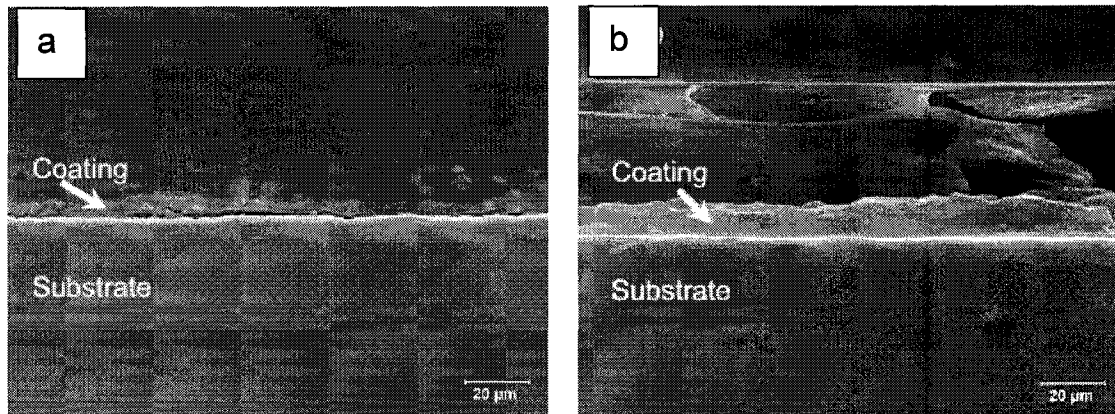


Figure 5. SEM micrograph of profile of coating on NPAS surface (a) and PMOD surface (b).

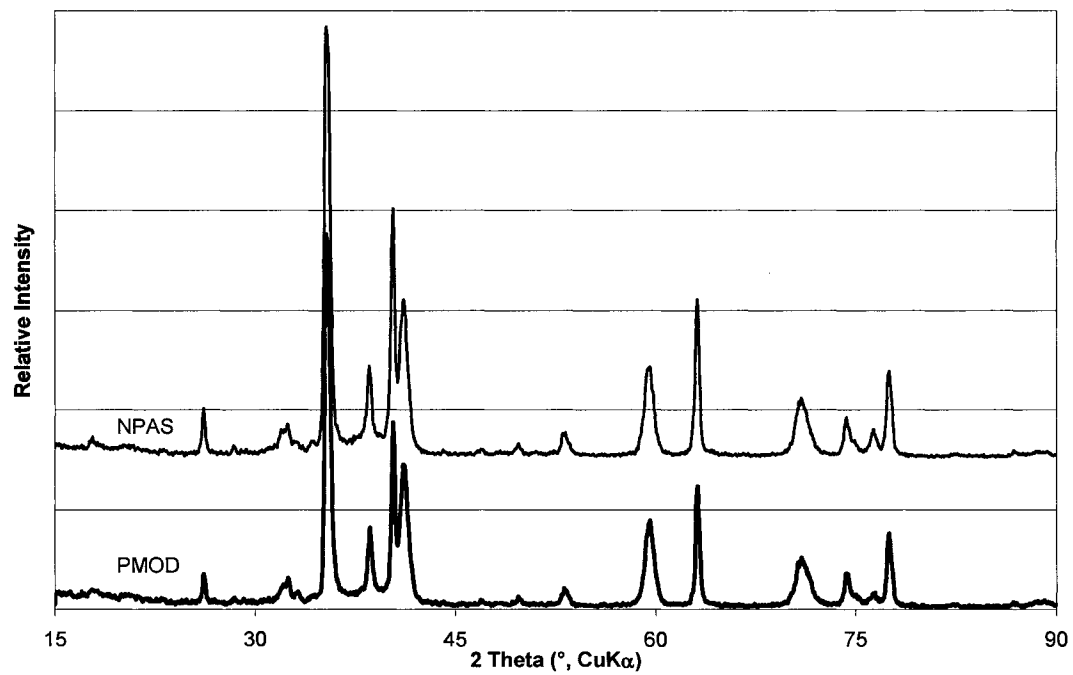


Figure 6. XRD scan of as-deposited ELD CaP coating on NPAS (top) and PMOD (bottom) titanium substrates

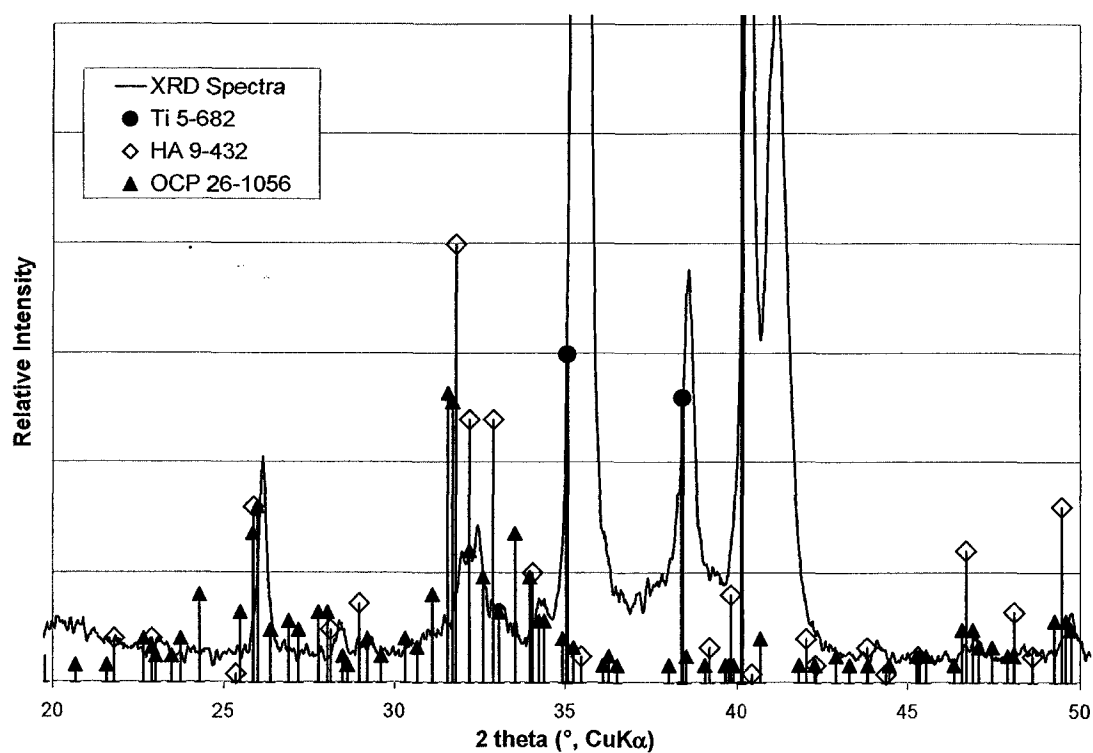


Figure 7. Representative XRD scan of as-deposited ELD CaP coating on NPAS with corresponding ICDD files.

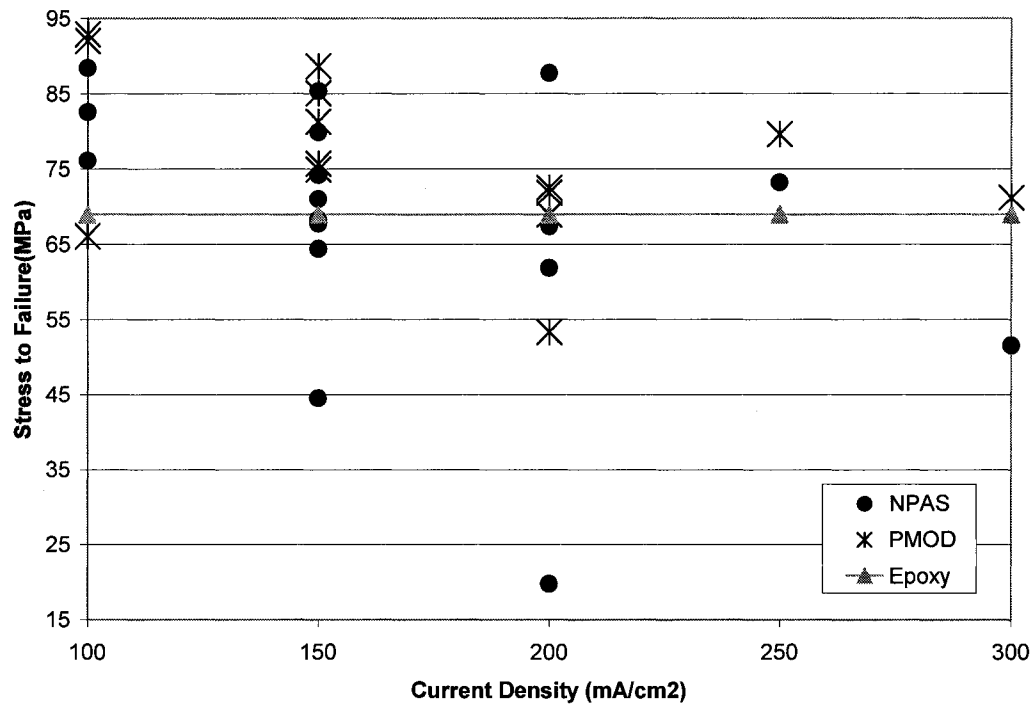


Figure 8. Bond strength of ELD CaP coated titanium deposited at different current densities.

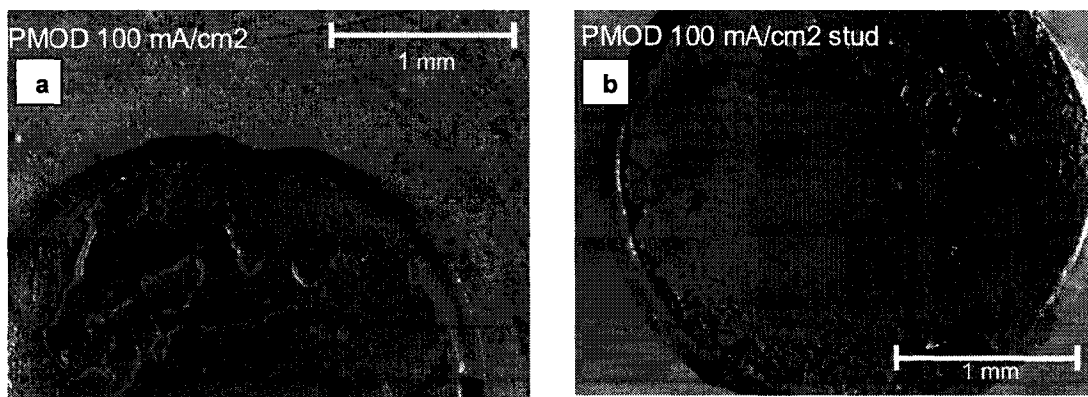


Figure 9. Representative images of coating surface (a) and corresponding stud surface (b) after adhesion test.

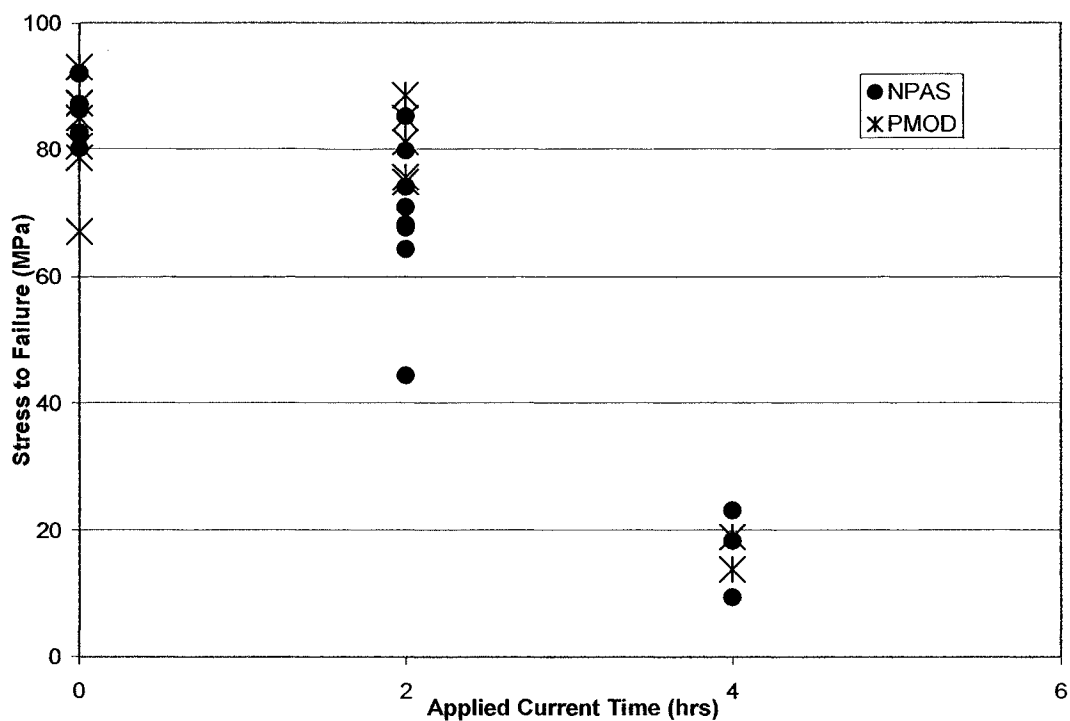


Figure 10. Bond strength of ELD CaP coating (150 mA/cm^2 deposition current density).

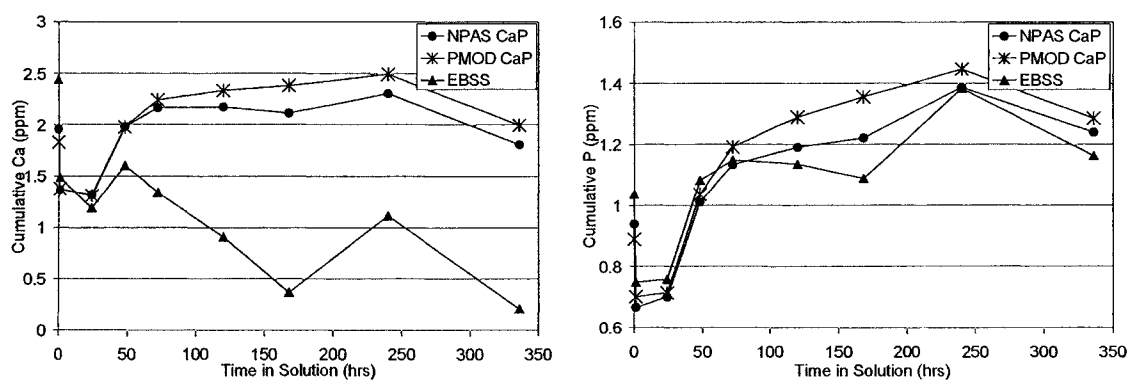


Figure 11. Cumulative change in solute calcium (left) and phosphorous (right) content over 14 day dissolution period.

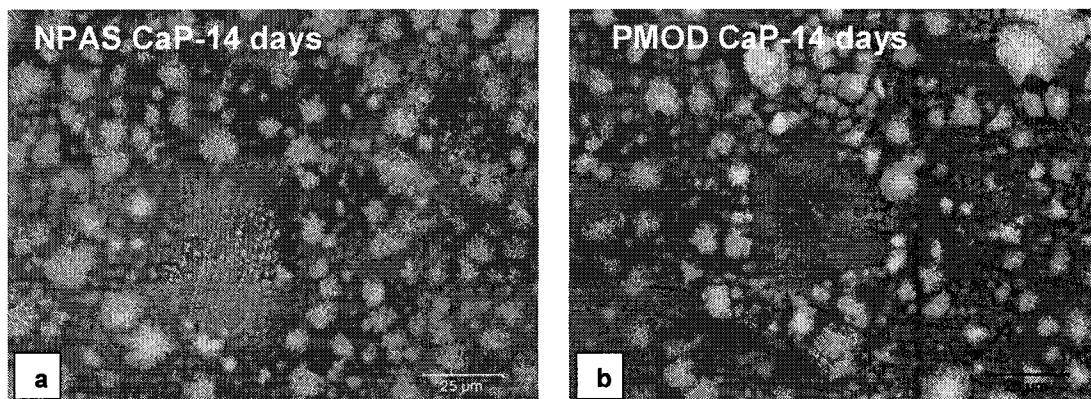


Figure 12. CaP Coatings after 14 days in Earle's Balanced Salt Solution on NPAS (a) and PMOD (b) treated substrates.

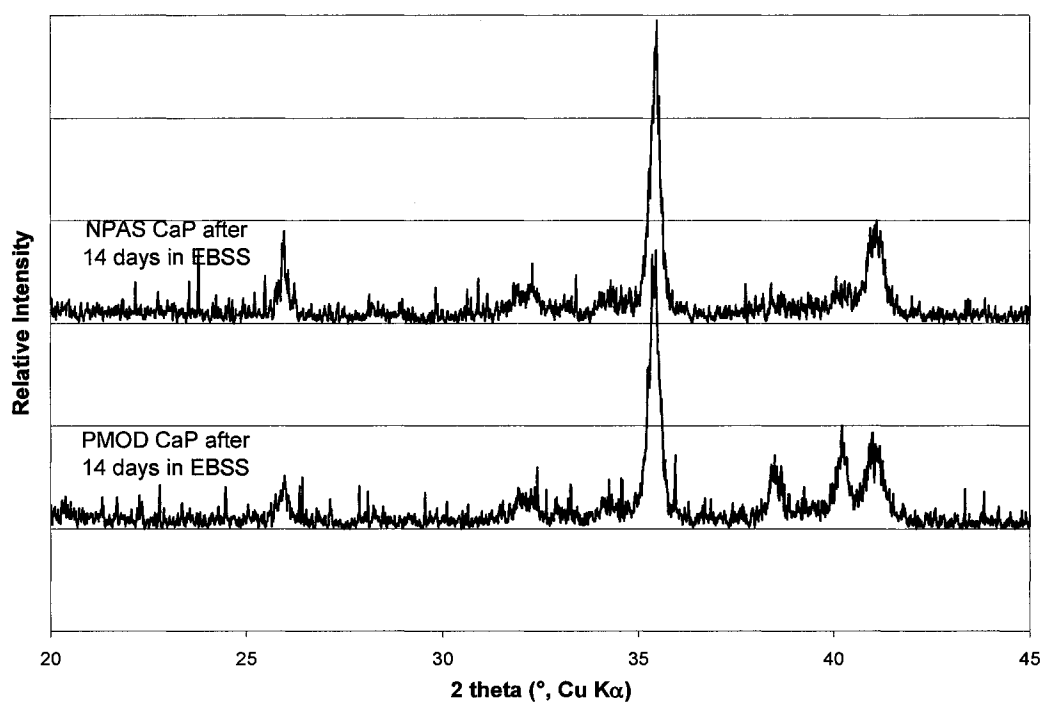


Figure 13. XRD of CaP coatings after 14 days in EBSS

ELECTROLYTIC DEPOSITION OF HYDROXLAPATITE USING A PULSED WAVE
TECHNIQUE

by

REBECCA SHUMATE O'CONNOR DAVIS, SUSAN L. BELLIS, RAMAKRISHNA
VENUGOPALAN, AND GREGG M. JANOWSKI

In preparation for *Journal of Biomedical Materials Research Part B: Applied
Biomaterials*

Format adapted for dissertation

ABSTRACT

Electrolytic deposition (ELD) is a novel technique that can be readily controlled to deposit a variety of calcium phosphate (CaP) coatings. The focus of this study was to deposit hydroxylapatite (HA) coatings using ELD and a simple unbuffered CaP electrolyte by incorporating the principles of solubility isotherms. A saturated CaP electrolyte was formulated to deposit HA on commercially pure titanium (cpTi) that had been either passivated in nitric acid (NPAS) or treated further by etching in phosphoric acid (PMOD). A symmetric pulsed square wave was used to apply the CaP coatings; frequency was optimized to get continuous coating coverage. More nucleation sites were seen on the ELD coated PMOD than NPAS; this was the only discernable difference between the two substrate treatments. SEM showed that ELD formed a continuous coating that mimicked the substrate topography. EDS, XRD, and FTIR showed good comparison between the ELD HA and bulk HA pellets. Bond strength of the ELD HA coatings were at or above most published values for CaP coatings. It was found that ELD is a controllable process that can deposit thin uniform HA coatings on cpTi.

INTRODUCTION

Calcium phosphates (CaP) have been used as biomaterials for over 20 years and are often used to coat titanium implants combining the favorable chemical properties of the ceramic with the mechanical properties of the substrate. These coatings have been shown to facilitate early bone integration for orthopedic and dental implants.¹⁻⁵ Plasma spraying is the most commonly used technique to apply CaP coatings, usually producing coatings containing several CaP phases, including hydroxylapatite (HA), β -tricalcium

phosphate, and amorphous calcium phosphate, due to the high temperature and rapid cooling during coating.⁶⁻⁹ The various CaP phases have different solubilities and can create sites of coating loss and subsequent coating failure upon implantation.⁸

Alternate coating methods have been explored in an attempt to overcome the limitations of plasma spraying. Ion beam sputtering and RF magnetron sputtering methods can produce CaP coatings but still require post heat treatments to improve crystallinity and to transform to the more stable HA phase.¹⁰⁻¹³ Coatings created by precipitation of CaP from saturated solutions can result in thin, uniform coatings on complex geometries. These immersion techniques have yielded bioactive CaP layers on titanium^{14,15} but can be very time consuming due to the induction times for nucleation and subsequent growth on the surfaces.^{16,17}

Electrolytic deposition (ELD) of CaP from solution on titanium substrates is a promising alternate method of thin coating preparation for biomedical implants. Unlike line-of-sight techniques such as plasma spraying or sputtering, ELD of CaP allows more control of the final coating chemistry, and a uniform crystalline coating of complex implant geometries and ELD requires less time to achieve micron thicknesses than immersion techniques. ELD deposits CaP by driving ions out of solution onto the cathode through hydrolysis reactions of metal ions and complexes in the electrolyte. CaP coatings have been deposited from solutions of $\text{Ca}(\text{NO}_3)_2$ and $\text{NH}_4\text{H}_2\text{PO}_4$ using ELD.¹⁸⁻²²

The objective of this study was to fabricate HA coatings and apply the principles of CaP solubility isotherms to ELD. A resorbable CaP was successfully deposited on commercially pure titanium (cpTi) with controlled solution conditions using an unbuffered CaP electrolyte.¹⁷ Briefly, an unbuffered, equimolar CaP containing electrolyte

successfully deposited a resorbable CaP on cpTi at low temperature with ELD. For the current study, ELD was used to deposit HA on cpTi by adjusting the applied deposition current, and the pH and Ca to P ratio of the unbuffered CaP electrolyte according to CaP solubility isotherms.^{23,24} Additionally, the effects of cpTi substrate surface modification on the ELD coating morphology and bond strength were investigated.

MATERIALS AND METHODS

Fabrication

Grade 2 cpTi disks ($\varnothing = 16$ mm) were wet ground through 600 grit SiC paper. The polished disks were cleaned and passivated per ASTM F86 guidelines: sonication in acetone, distilled water, ethanol, and distilled water, and soaking in 30% nitric acid for 20 minutes (NPAS). Half of the substrates were treated further by immersion in 30% phosphoric acid for 20 minutes (PMOD).

An electrolytic bath with 1.00×10^{-3} M concentration of Ca^{2+} and 6.10×10^{-4} M concentration of PO_4^{3-} was formulated to deposit hydroxylapatite (HA) based upon solubility isotherms and associated Gibb's Free Energy of calcium phosphate phases. Reagent grade NaCl, CaCl_2 , KH_2PO_4 , and KOH were used for the electrolyte; the starting pH was 6.5 ± 0.1 with a 0.15 M total ionic activity. A fresh bath was used for each deposition. The coating deposition is attributed to three reaction stages that take place at the cathode, found in Table 1.²¹

TABLE 1. Summary of cathodic reactions during ELD of CaP.

Cathodic reaction	Process	Open circuit voltage
$O_2 + 2H_2O + 4e^- \rightarrow 4OH^-$	reduction of oxygen	-0.4 V
$2H_2PO_4^- + 2e^- \rightarrow 2H_2PO_4^{2-} + H_2$	reduction of acid phosphate	-0.4 to -1.6 V
$H_2PO_4^{2-} + 2e^- \rightarrow 2PO_4^{3-} + H_2$		
$2H_2O + 2e^- \rightarrow H_2 + 2OH^-$	reduction of water	-1.6 to -3.0 V

All experiments were performed in double-walled glass vessels at 37°C purged with humidified nitrogen to remove oxygen and deter $CaCO_3$ formation. A power source was connected to the cpTi substrate (cathode) and a Pt/Nb wire mesh (anode) as shown in the schematic of Figure 1. Substrates were exposed to either a constant or pulsed current during deposition. For constant current deposition, a Hewlett Packard 6633A System DC power supply was used. The disks were exposed to a current density of 100, 150, 200, or 300 mA/cm² for 2 hours. A BK Precision Model 4011 5 MHz Sweep/Function Generator was used to apply a symmetric square wave at frequencies ranging from 0.5 to 10 Hz for 4 h. DC offset and output were set at maximum values for the function generator resulting in applied current densities of 4 and 200 mA/cm² (0.64 and 7.00 V, respectively) each cycle (see Figure 2). Bath temperature and pH were measured before and after all depositions to monitor consistency; this data was also useful in interpreting phase formation. The coated substrates were then rinsed with distilled water and ethanol, dried with a heat gun on low setting, and stored in a desiccator until further analysis.

Bulk HA disks were used as comparison to the ELD coated Ti disks. Commercially available HA powder (Fisher) was pressed to form 16 mm diameter unsintered pellets (HAU) in a hardened steel die using approximately 27.6 MPa of pressure. The HAU disks were then sintered at 1000°C for 3 h (HAS).

Characterization

X-ray Diffraction

X-ray diffraction (XRD) was used to identify the calcium phosphate phase in the coating. The scans used a $0.02^\circ 2\theta$ step size for 6 s/step over a $30\text{--}70^\circ 2\theta$ range and a $\text{CrK}\alpha$ radiation source (40 keV, 30 mA). The scans were converted to $\text{CuK}\alpha$ for comparison with other published data. ELD coating spectra were compared with International Centre for Diffraction Data (ICDD) files as well as spectra of known bulk HA samples, HAU and HAS.

Scanning Electron Microscopy/ Electron Dispersive Spectroscopy

SEM was used to examine the morphology of the substrates, ELD coated disks (both NPAS and PMOD), and bulk HA using an accelerating voltage of 30 keV. The samples were cleaned in methanol before sputter coating with gold and palladium for analysis. EDS was also performed using a 500X scan area and standardless quantification methods using 15 keV on the ELD coatings, HAU, and HAS; the lower voltage was used to minimize excitation of the Ti substrate.

X-ray Photoelectron Spectroscopy

X-ray photoelectron spectroscopy (XPS) was performed using a monochromatic Al (1487 eV) x-ray source that penetrated less than 5 nm into the surface. High-resolution scans were performed at 40 eV for 3 samples of each of the following groups: uncoated NPAS, uncoated PMOD, and coated NPAS. Curve fitting of spectra was performed using Spectral Data Processor v3.0.

Fourier Transform Infrared Spectroscopy

Samples were examined Fourier Transform Infrared Spectroscopy (FTIR) to determine the presence of functional groups. The instrument was operated in reflectance mode and surveyed from 400 to 4000 cm^{-1} using 32 scans with 4 cm^{-1} resolution.

Coating bond strength

Epoxy coated studs were affixed to the ELD coatings, and the normal stress required to detach the stud from the sample surface was measured. Studs were affixed with a clamp and cured for 1 h at 150°C to ensure mounting perpendicular to the surface. After cooling, the samples were tested using a Sebastian Five Strength Tester (Quad Group). Samples were loaded at a rate of 5 kg/s until failure. After testing, samples and studs were visually inspected using stereomicroscopy.

RESULTS AND DISCUSSION

Substrate Treatment

The substrates were examined using several characterization techniques to determine what, if any, effects the different acid preparation had on the Ti surfaces. XRD indicated that the cpTi (ICDD 5-682) had a (0 0 2) texture. The spectra of the uncoated NPAS and PMOD cpTi were indistinguishable (Figure 3). Carbon, oxygen, nitrogen, and titanium were detected using XPS on the surfaces of both treatment groups, but phosphorus was found only on the PMOD cpTi surfaces, indicating a difference in the surface chemistries of the cpTi disks. The surface morphologies were indistinguishable on SEM, having similar roughness and topography.

Deposition Parameters

Constant current deposition was attempted at current densities between 100 and 300 mA/cm² which resulted in poor coverage of the substrates for both substrate treatments. Nucleation sites were poorly dispersed and large agglomerates were not connected to other coating areas, illustrated by a representative sample in Figure 4. Precipitates were found in the baths as well. This observation can be explained by the buildup of OH⁻ at the cpTi cathode surface (see Table 1) as found in other ELD research.²⁰⁻²² The higher concentration of OH⁻ at the substrate surface results in a gradual, localized increase in pH from the bulk electrolyte to the substrate, illustrated in Figure 5.²⁰ As the ions from the bulk electrolyte approach the surface, the increase in pH drives the precipitate out into solution.

Pulsed deposition was investigated in an attempt to deposit a more continuous coating. The pulsed current shown in Figure 2 was applied to overcome the large difference in size and mobility of the Ca^{2+} and PO_4^{3-} ions in the electrolytic bath. To parallel the time of cathodic polarization used for the 2-h constant current, the square wave was applied for 4 hours (a total of 2 h on and 2 h off). The off time allowed the larger, slower PO_4^{3-} ions to travel to the surface of the Ti cathode and bond with the Ca^{2+} ions already present on the surface.²⁵ This time without the applied current minimized the diffusion layer (shown in Figure 5) at the cathode, reducing the OH^- concentration at the substrate, and enabling anions to bond to the cations at the proper stoichiometry for deposition of HA.

Depositions were performed on NPAS and PMOD cpTi substrates for the preliminary studies at the following frequencies: 0.5, 1.0, 2.0, and 10.0 Hz. Coatings deposited at 2 Hz were uniform and continuous, while those deposited at the other frequencies were not for either substrate treatment (see Figure 6). Frequencies less than 2 Hz produced coatings that did not cover the cpTi surface; nucleation sites were dispersed. Coatings deposited at 10 Hz produced precipitate in the electrolyte and were very similar to those deposited using constant current. The voltage transient was measured across the electrochemical cell set at the initial dc offset and output; there was no transient seen. The system was operating well below the critical frequency; therefore ion mobility was the rate limiting effect occurring at the electrode. A 2.0 ± 0.5 Hz square wave was used for the remaining experiments. The pH at the end of the deposition was 6.9 ± 0.1 .

Coating Characterization

To investigate the early stages of the deposition, ELD coated cpTi disks were sonicated in methanol for 2 min. As seen in Figure 7, there are visibly more nucleation sites on the ELD coated PMOD (b) than on the ELD coated NPAS (a) cpTi substrate after the sonication. This difference between cpTi acid treatments did not translate to the morphology of the as-deposited coating, which indicates that growth is able to compensate for the initial difference in nucleation sites.

The topography of the substrate was mimicked through the ELD coatings. No significant differences were seen when comparing the NPAS and PMOD ELD coatings. Coatings appeared to be approximately 10 microns thick having particle sizes ranging from 5 to 15 microns, illustrated in Figure 8.

EDS was performed to quantify the Ca to P ratio of the ELD coatings and bulk HA. EDS revealed ratios for the ELD coatings (ELD NPAS = 1.54 ± 0.22 , ELD PMOD = 1.53 ± 0.12) were higher than those for the bulk HA disks (HAU = 1.38 ± 0.04 , HAS = 1.39 ± 0.04). This discrepancy could be attributed in part to the higher detection of carbon compared to the ELD coatings.

Crystal structure was investigated using XRD on the ELD coated NPAS and PMOD disks, HAU, and HAS. Substrate treatment had no effect on the ELD coatings; spectra were indistinguishable. Sintering of the HA disks increased the crystallinity of the HAS disks compared to HAU disks; HAS disks had well defined peaks. Figure 9 shows that there was good agreement for all spectra with the ICDD file for HA (9-0432) and titanium (05-682) on the ELD coated disks. The ELD coatings had a predominantly (002) texture at $26^\circ 2\theta$. A search was performed for CaP ICDD files that corresponded to the

visible peak around $41^\circ 2\theta$ in the ELD coating but no CaP was found to include a peak for that 2θ . This unknown could also have contributed to the higher EDS of the ELD compared to the bulk HA.

XPS was performed on ELD coated NPAS cpTi disks to characterize the surface of ELD coatings. No titanium was detected, supporting the SEM images of continuous coatings. High resolution scans gave calcium to phosphorous ratio of 1.23 ± 0.05 for the coatings deposited on NPAS titanium disks.

FTIR was performed to investigate the functional groups present on the surface of the samples. There was good agreement of the ELD coatings with both HAU and HAS disks as can be seen in Figure 10. Bands derived from the PO_4 modes for HA sited in other works correlated well with those observed in this study (1090, 1020, 962, 600, and 563 cm^{-1}).¹⁹ No bands associated with carbonate ions were detected in any of the ELD coatings. The characteristic large, sharp peak from the stretching mode of hydroxyl groups around 3570 cm^{-1} usually seen with HA^{18,19,26} was not pronounced in any of the spectra. While there was a slight peak, the absence of intensity was attributed to signal loss during collection. Samples were placed externally on a crystal while collecting the spectra in reflectance mode. The roughness of the sample surface against the smooth crystal allowed for some possible absorption or deflection of the signal during collection.

Bond Strength

Bond strength tests were performed on the ELD coated Ti disks to investigate the adhesion strength of the coating to the Ti substrate. It was thought that the presence of phosphorous on the PMOD cpTi surface would provide both better and more bonding

sites for the CaP coating which would lead to higher coating bond strength. As seen in Figure 7, there were more nucleation sites on the ELD PMOD cpTi than the ELD NPAS cpTi after being sonicated for 2 min. The ELD coating was better attached to the PMOD in that there was more coating present than on the NPAS. This visible difference in attachment of the coating in the early stage of deposition did not translate to a quantifiable difference of the final ELD coating on the two different cpTi acid treatments. ELD NPAS coatings had bond strengths of 60.81 ± 11.60 MPa, while PMOD had 62.28 ± 19.61 MPa. While the difference was not statistically significant, both groups had high values, at or above most published values for similar coatings. Failures all occurred within the epoxy or at the coating/substrate interface; none were within the coating.

CONCLUSIONS

1. Ti substrate surface chemistry was altered by exposure to different acids. This did not lead to detectable differences in the characterization of the applied coatings.
2. ELD in a neutral CaP containing electrolyte formulated to deposit HA (Ca:P = 1.67) required the application of a pulsed square wave. ELD coatings deposited by pulsed deposition were optimized at 2 Hz, resulting in continuous coverage of the cpTi.
3. Crystal structure, morphology, chemistry and bond strength of applied ELD coatings were unaffected by substrate surface treatments.
4. ELD coatings were comparable to commercially available bulk HA in terms of XRD and FTIR, as well as ICDD file 9-432 for HA.
5. ELD HA coatings had high bond strengths.

6. HA coatings were fabricated on cpTi by ELD using a simple electrolytic bath at 37°C without post heat treatment.
7. The formulation of the unbuffered CaP electrolyte can be adapted to deposit different phases of CaP using ELD.

ACKNOWLEDGEMENTS

The authors would like to thank Dr. Earl T. Ada for his assistance with training and analysis on the XPS in the Surface Analysis Laboratory at the University of Alabama, Tuscaloosa, AL. Additionally, we would like to acknowledge Dr. Derrick Dean for providing FTIR data and Ms. Amber Sawyer for preparing the pressed HA pellets.

REFERENCES

1. Jarcho M. Calcium phosphate ceramics as hard tissue prosthetics. *Clinical Orthopaedics and Related Research* 1981;157:257-278.
2. Ducheyne P, Hench LL, Kagan A, Martens M, Burssens A, Mulier JC. The effect of hydroxyapatite impregnation on skeletal bonding of porous coated implants. *Journal of Biomedical Materials Research* 1980;14:225-237.
3. Cook SD, Thomas KA, Dalton JF, Volkman TK, Whitecloud TS, Kay JF. Hydroxylapatite coatings of porous implants improves bone ingrowth and interface attachment strength. *Journal of Biomedical Materials Research* 1992;26:989-1001.
4. Cook SD, Thomas KA, Kay JF, Jarcho M. Hydroxyapatite-coated porous titanium for use as an orthopedic biologic attachment system. *Clinical Orthopaedics and Related Research* 1988;230:303-312.
5. Rivero DP, Fox J, Skipor AK, Urban RM, Galante JO. Calcium phosphate-coated porous titanium implants for enhanced skeletal fixation. *Journal of Biomedical Materials Research* 1988;22:191-202.

6. Lucas LC, Lacefield WR, Ong JL, Whitehead RY. Calcium phosphate coatings for medical and dental implants. *Colloids and Surfaces A: Physicochemical and Engineering Aspects* 1993;77:141-147.
7. Wang BC, Chang E, Lee TM, Yang CY. Changes in phases and crystallinity of plasma-sprayed hydroxyapatite coatings under heat treatment: A quantitative study. *Journal of Biomedical Materials Research* 1995;29:1483-1492.
8. Radin SR, Ducheyne P. Plasma spraying induced changes of calcium phosphate ceramic characteristics and the effect on *in vitro* stability. *Journal of Materials Science: Materials in Medicine* 1992;3:33-42.
9. McPherson R, Gane N, Bastow TJ. Structural characterization of plasma-sprayed hydroxylapatite coatings. *Journal of Materials Science: Materials in Medicine* 1995;6:327-334.
10. Ong JL, Lucas LC. Post-deposition heat treatments for ion beam sputter deposited calcium phosphate coatings. *Biomaterials* 1994;15:337-341.
11. Zeng H. Evaluation of bioceramic coatings produced by pulsed laser deposition and ion beam sputtering [Dissertation]. Birmingham, AL: University of Alabama at Birmingham; 1997.
12. Jansen JA, Wolke JG, Swann S, van der Waerden JP, de Groot K. Application of magnetron sputtering for producing ceramic coatings on implant materials. *Clinical Oral Implants Research* 1993;4:28-34.
13. Ratner BD, Hoffman AS, Schoen FJ, Lemons JE, editors. *Biomaterials science: an introduction to materials in medicine*. San Diego: Academic Press; 1996.
14. Wen HB, Wolke JG, de Wijn JR, Liu Q, Cui FZ, de Groot K. Fast precipitation of calcium phosphate layers on titanium induced by simple chemical treatments. *Biomaterials* 1997;18(22):1471-1478.
15. Li P, Matthews F. The solution-induced three-dimensional transformation of porous titanium ingrowth surfaces into a carbonated apatite for enhancing bone ingrowth and attachment. Presented at 45th Annual Meeting, Orthopedic Research Society, Anaheim, California 1999.

16. Wu W, Nancollas GH. Nucleation and crystal growth of octacalcium phosphate on titanium oxide surfaces. *Langmuir* 1997;13:861-865.
17. O'Connor RS, Burke EB, Lucas LC. Effect of Titanium Surface Treatments on Controlled Calcium Phosphate Precipitation. *Critical Reviews in Biomedical Engineering* 1999;26(5-6):293-447.
18. Shirkhanzadeh M. Electrochemical preparation of bioactive calcium phosphate coatings on porous substrates by the periodic pulse technique. *Journal of Materials Science Letters* 1993;12:16-19.
19. Shirkhanzadeh M. Calcium phosphate coatings prepared by electrocrystallization from aqueous electrolytes. *Journal of Materials Science: Materials in Medicine* 1995;6:90-93.
20. Shirkhanzadeh M. Direct formation of nanophase hydroxyapatite on cathodically polarized electrodes. *Journal of Materials Science: Materials in Medicine* 1998;9:67-72.
21. Kuo MC, Yen SK. The process of electrochemical deposited hydroxyapatite coatings on biomedical titanium at room temperature. *Materials Science and Engineering C* 2002;20:153-160.
22. Yen SK, Lin CM. Cathodic reactions of electrolytic hydroxyapatite coating on pure titanium. *Materials Chemistry and Physics* 2002;77:70-76.
23. Brown WE, Chow LC, inventors; American Dental Association Health Foundation, assignee. Dental restorative cement pastes. United States patent 4518430. 1985 May 21.
24. Johnsson MS, Nancollas GH. The role of brushite and octacalcium phosphate in apatite formation. *Critical Reviews in Oral Biology and Medicine* 1992;3(1-2):61-82.
25. Lin S, LeGeros RZ, LeGeros JP. Adherent octacalciumphosphate coating on titanium alloy using modulated electrochemical deposition method. *Journal of Biomedical Materials Research* 2003;66A:819-828.

26. Baddiel CB, Berry EE. Spectra structure correlations in hydroxy and fluorapatite. *Spectrochimica Acta* 1966;22:1407-1416.

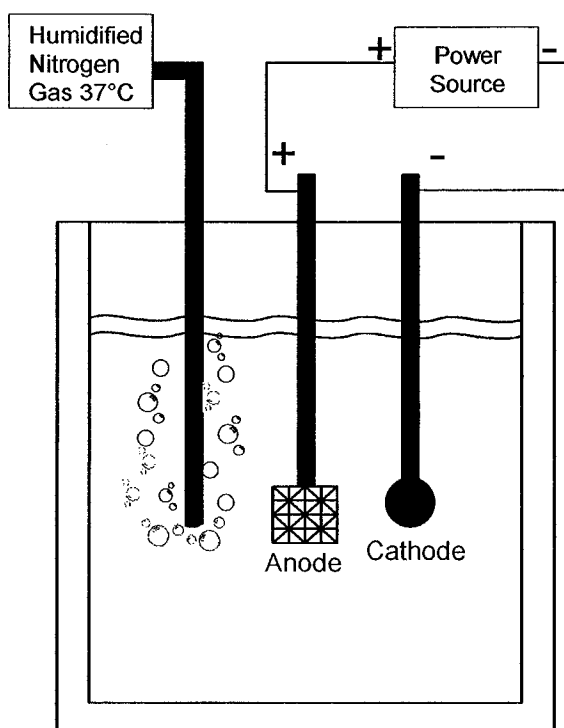


Figure 1. Electrochemical deposition cell showing major components.

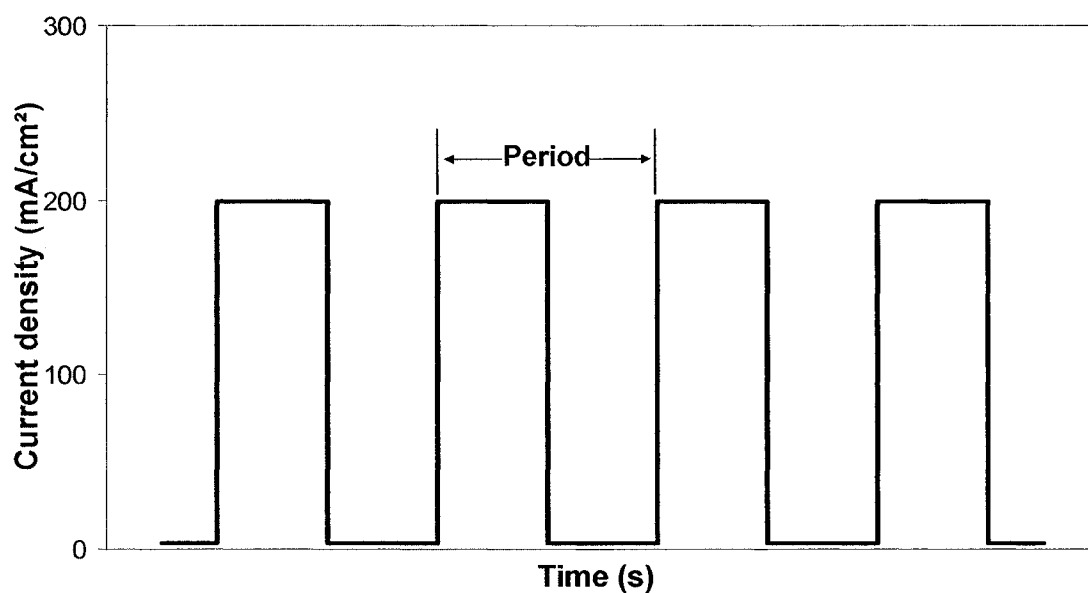


Figure 2. Representation of applied current for pulse deposition experiments. Periods were between 0.1 s (10 Hz) and 2.0 s (0.5 Hz). The maximum and minimum current densities ranged from 196 to 200 mA/cm² and 0 to 4 mA/cm², respectively.

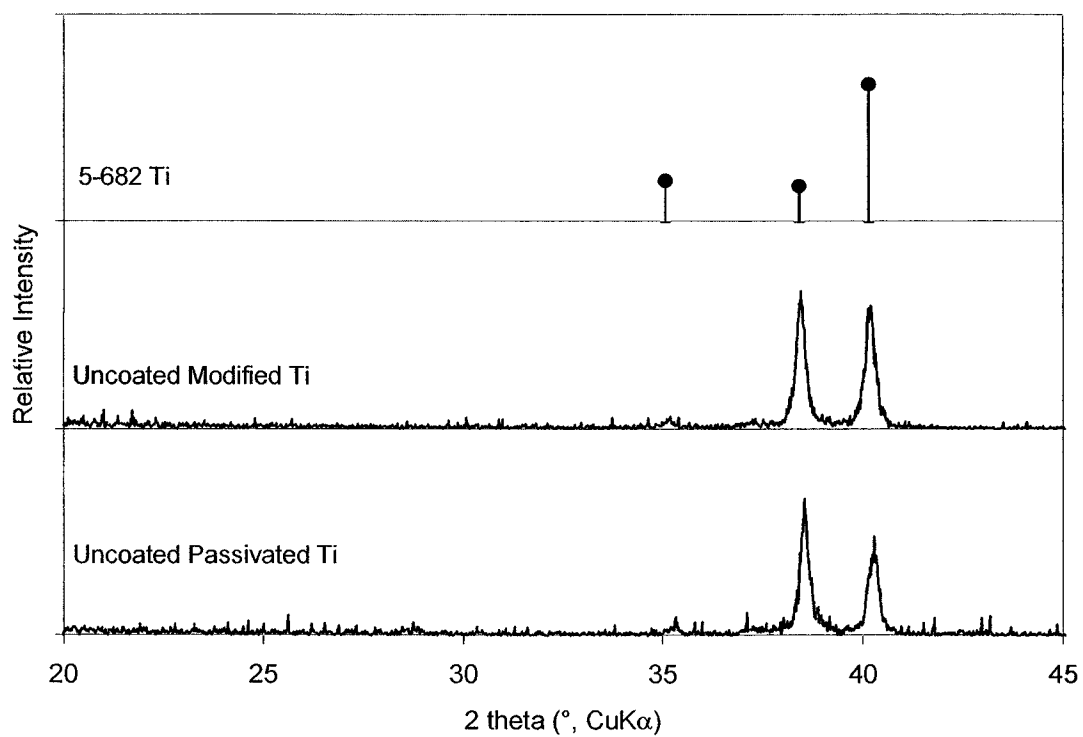


Figure 3. XRD Spectra of uncoated NPAS and PMOD cpTi substrates show agreement with ICDD file 5-682 for titanium having a (0 0 2) texture.



Figure 4. Representative SEM image of ELD CaP coating deposited using constant current density (200 mA/cm^2 on NPAS cpTi substrate).

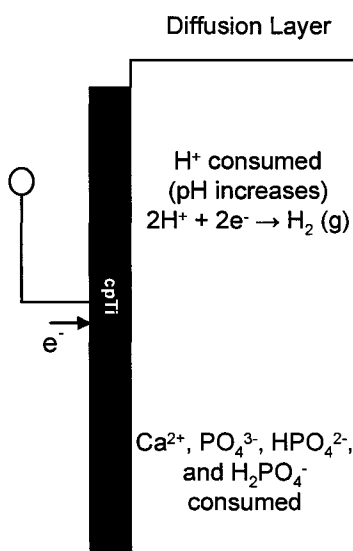


Figure 5. Schematic of reaction at cathode.

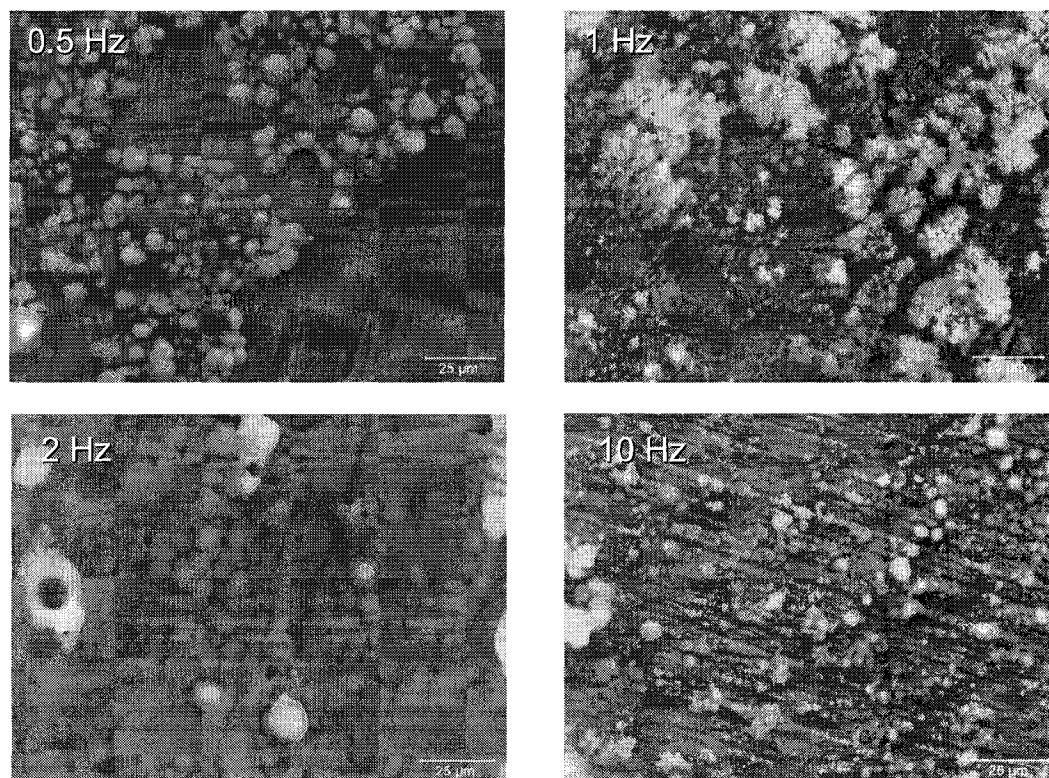


Figure 6. ELD coatings on NPAS substrates deposited at different frequencies. A continuous coating was deposited using 2 Hz square wave. Calibration mark is 25μm.

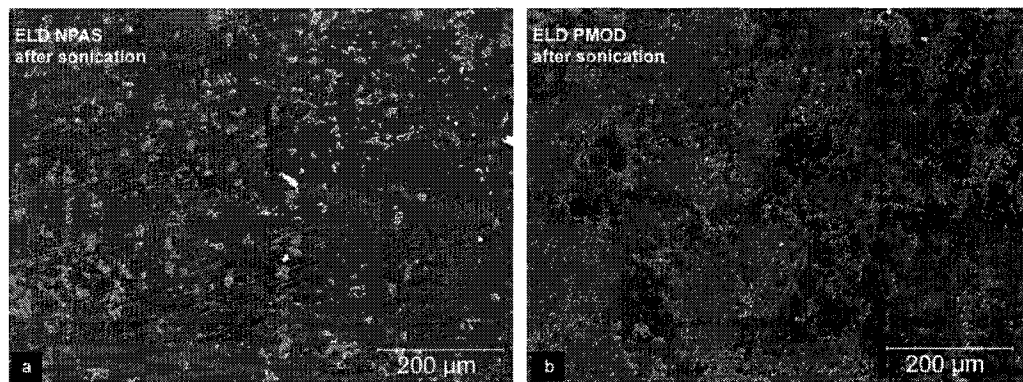


Figure 7. ELD coated cpTi NPAS (a) and PMOD (b) after placing in an ultrasonic cleaner with methanol for 2 minutes. There are more visible nucleation sites on the ELD PMOD surface.

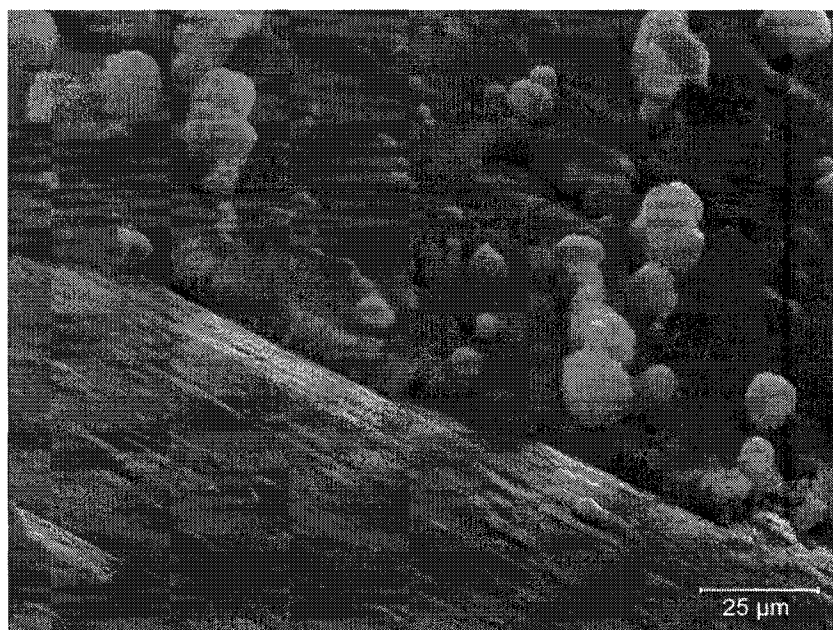


Figure 8. Edge of ELD coating on Ti substrate illustrating coating thickness.

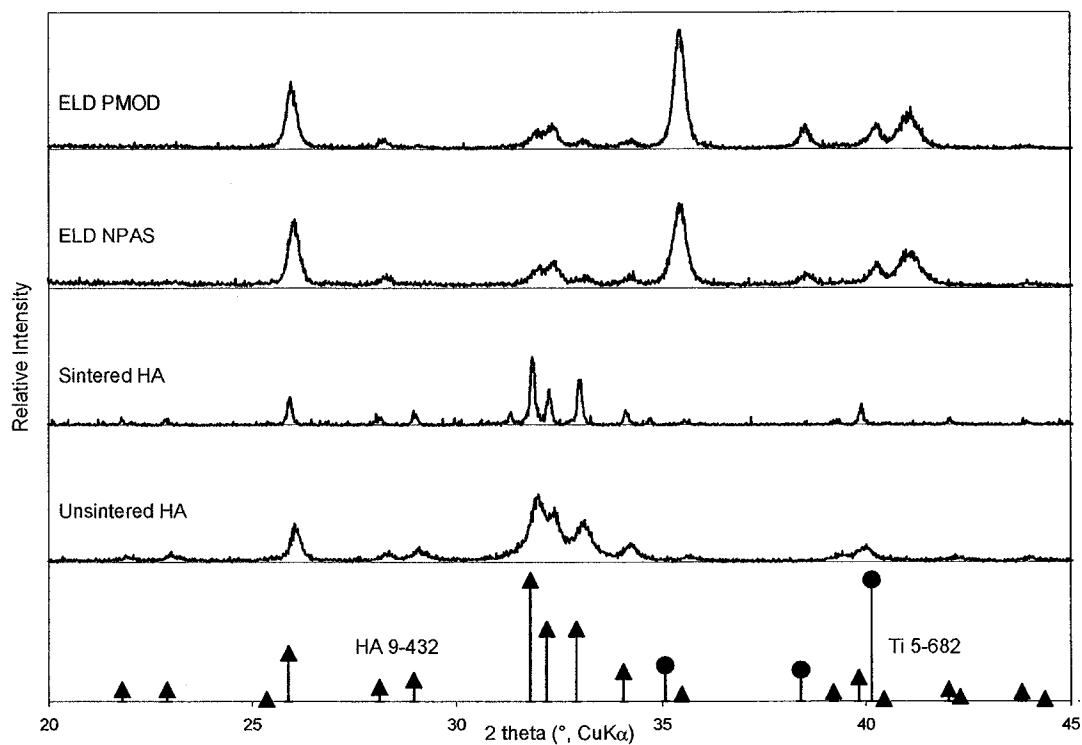


Figure 9. XRD spectra of as-deposited ELD HA coatings on ELD NPAS and PMOD cpTi substrates compared to ICDD files and bulk HA (HAU and HAS).

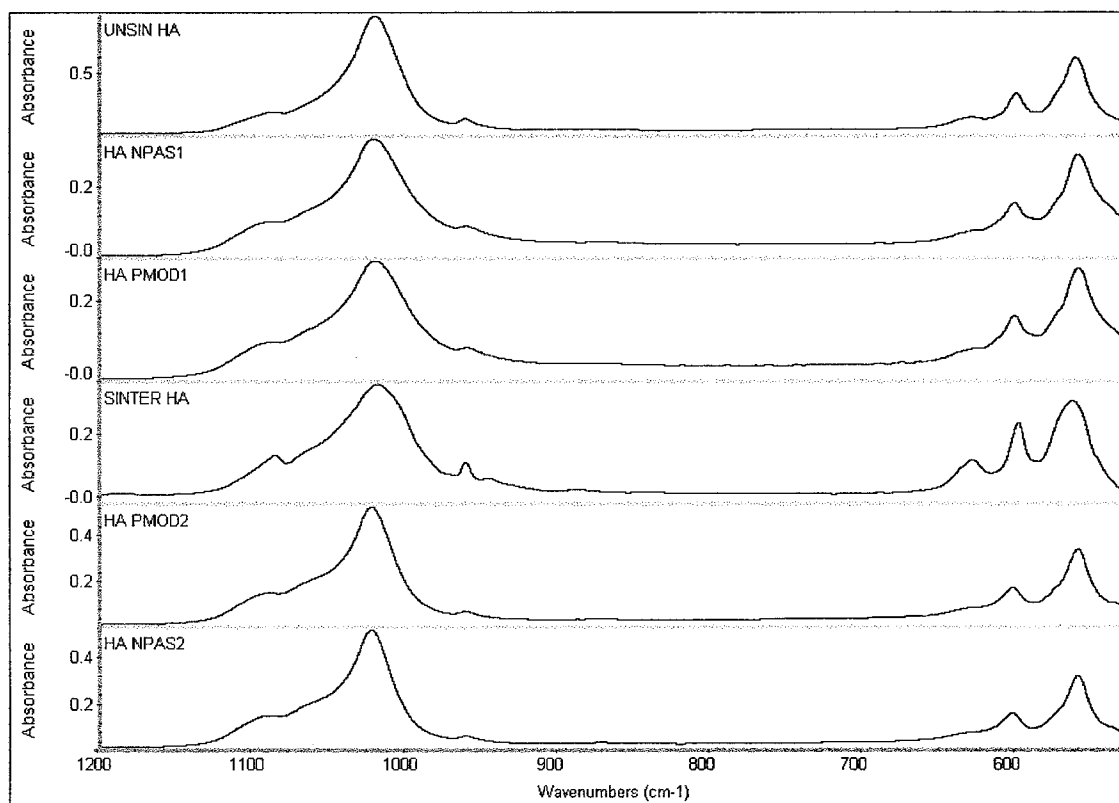


Figure 10. FTIR spectra reflects similarities between the ELD deposited coatings on cpTi and pressed HA pellets.

DISSOLUTION AND CELLULAR BEHAVIOR OF ELECTROLYTICALLY
DEPOSITED HYDROXYLAPATITE

by

REBECCA SHUMATE O'CONNOR DAVIS, GREGG M. JANOWSKI,
RAMAKRISHNA VENUGOPALAN, AMBER A. SAWYER, AND SUSAN L. BELLIS

In preparation for *Journal of Materials Science: Materials in Medicine*

Format adapted for dissertation

ABSTRACT

Hydroxylapatite (HA) coatings are used on dental and orthopedic implants to enhance the bond of the implant with the surrounding bone and improve implant stability through osteoconduction. The reported osteoconduction of HA has been investigated on many levels, from overall implant performance *in vivo*, to studies of cell signaling on materials surfaces *in vitro*. The purpose of this study was to evaluate the biocompatibility of HA coatings fabricated using electrolytic deposition (ELD). The dissolution behavior of ELD HA coated Ti disks was compared to that of sintered HA pellets using Earle's Balanced Salt Solution (EBSS). SEM, EDS, XRD, and FTIR were performed before and after dissolution. Human mesenchymal stem cells (MSC) were seeded on ELD HA coated and uncoated Ti disks with and without the presence of serum. ELD HA was comparable to the sintered HA pellets in terms of characterization and solubility; Ca and P came out of the EBSS and deposited on both surfaces. MSCs required serum to spread on all surfaces, a result that is consistent with previous studies of MSC behavior on sintered HA. In light of these studies, it was concluded that ELD HA has good potential for use as a biocompatible coating.

INTRODUCTION

Hydroxylapatite (HA, $\text{Ca}_{10}(\text{PO}_4)_6(\text{OH})_2$) is a calcium phosphate (CaP) that most resembles the mineral phase that composes bone. HA has been shown to promote bone growth when placed in the body, a function deemed osteoconductive.¹ Its use as a coating on orthopedic and dental implants enables the combination of good mechanical properties of the underlying metal substrate with the bioactive surface of HA.¹⁻⁴ HA is in intimate

contact with bone; with time, bone attaches to the HA through a thin ($<0.2\ \mu\text{m}$) epitaxial bonding layer containing bone minerals.^{1,5,6} This bond allows good fixation and overall function of the implant.

The osteoconductive behavior of HA is due to its reactions in aqueous solution where CaP is in a dynamic equilibrium. Dissolution and reprecipitation of Ca^{2+} and PO_4^{3-} occurs at the surface, pulling ions from the surface and surrounding environment. This exchange of ions can create local saturation which changes the local pH and results in precipitation of other CaP phases on the surface. The resulting phase is dependent on the pH, ionic concentrations, and temperature, and may be different from the original coating. As can be seen by the solubility isotherm in Figure 1, HA is the most thermodynamically stable CaP phase in neutral pH conditions and usually forms when CaP is precipitated from solutions in this range. Biocompatible CaP phases, including dicalcium phosphate dihydrate (DCPD) and octacalcium phosphate (OCP), have been shown to convert to HA when placed in neutral calcium and phosphate containing saline solutions at 37°C , conditions that mimic the biological environment.⁷⁻⁹

Ceramic and metallic surfaces placed in biological environments adsorb proteins. The amount and type of protein adsorption is dependent upon the physicochemical properties of the exposed material. Protein adsorption is driven by the bulk concentration and surface activity of the protein resulting in varying protein composition on different surfaces.¹⁰ CaPs, including HA, have been shown to adsorb more proteins as compared to titanium and stainless steel,¹¹⁻¹³ which translated to better attachment of osteoprogenitor cells to the material surface.¹¹ Studies consistently find more bone induction by HA compared to titanium alone. A study by ter Brugge found more $\alpha 5$, $\alpha 6$, and $\beta 1$ integrin ex-

pression on CaP.¹⁴ The presence of increased levels of the fibronectin-specific $\alpha 5 \beta 1$ integrin receptor could contribute to enhanced mineralization on CaP biomaterials, given that this receptor has been implicated in the osteoblastic differentiation of osteoprogenitor cells.¹⁵

Orthopedic and dental implants are covered in blood, adsorbing proteins on the surfaces, when placed in bone. Protein detachment does not easily occur; in effect, the proteins are immobilized on the surface once they are adsorbed.¹⁰ Certain proteins that are abundant in blood, particularly fibronectin and vitronectin, bind to cell surface integrins, which in turn tethers the cells to the implant surface. Mesenchymal stem cells (MSC), the cells of interest, have been shown to differentiate into bone cells when placed in the proper environment.¹⁶ This attachment of the MSC is thought to be a critical step in the overall bonding and incorporation of the implant in bone.

Electrolytic deposition (ELD) is a relatively simple and inexpensive method used to apply coatings by driving ions and complexes out of the electrolytic bath. It is a non-line-of-site technique capable of depositing HA on complex surface geometries, typical of biomedical implants.¹⁷⁻²⁰ *In vitro* experiments have shown good spreading and proliferation of osteoblastic cells on CaP coatings deposited using ELD²¹ while *in vivo* experiments have shown enhanced bone formation and subsequent increase of bone pull-out bond strengths of ELD CaP coated surfaces.²² HA has been shown to adsorb more serum proteins than titanium and have better binding of osteoblast precursor cells.¹¹ The focus of this study was to investigate the solubility of HA coatings deposited on titanium substrates using this novel technique and the behavior of MSCs on ELD HA coated and uncoated titanium substrates.

MATERIALS AND METHODS

Fabrication

Commercially pure titanium (cpTi) disks were wet ground through 600 grit using silicon carbide paper. The disks were then cleaned and passivated per ASTM F-86 standards: ultrasonically cleaned in acetone for 10 min, rinsed with distilled water, ultrasonically cleaned in ethanol for 10 min, rinsed with distilled water, statically passivated in 30% nitric acid for 20 min, rinsed with distilled water and then ethanol, and stored in a desiccator until use (NPAS). Some disks were treated further by etching in 30% phosphoric acid for 20 min, and then rinsed with distilled water followed by ethanol, and placed in a desiccator until use (PMOD).

Methods employed in this study to deposit HA using ELD are described elsewhere.¹⁷ Briefly, each disk was placed in sealed PTFE holders that masked the disk to 1 cm² exposed surface area. Each was then placed in a calcium and phosphorous containing electrolytic bath formulated to deposit HA based on the solubility isotherms in Figure 1. A 1 L double-walled beaker purged with humidified nitrogen was used for the electrochemical cell. The temperature of the beaker and nitrogen were maintained by a water bath held at 37°C. A function generator was connected to the cpTi cathode and a Pt/Nb wire mesh anode. A pulsed square wave was applied with current densities of 4 or 200 mA/cm² at 2.0 ± 0.1 Hz frequency for 4 h. Bath temperature and pH were monitored before and after deposition. At the end of the 4 h, each disk was removed and rinsed with distilled water followed by ethanol, dried with a heat gun on low setting, and stored in a desiccator.

Pellets of HA were made for comparison to the ELD HA coatings. Procedures set out by Sawyer et al.²³ were followed using commercially available HA powder (Fisher Scientific). Briefly, the powder was pressed using a 16 mm diameter steel die at approximately 20.7 MPa of pressure. The pellets were removed from the die and then sintered at 1000°C degrees for 3 h. The sintered HA pellets were allowed to cool and then stored in a desiccator.

Characterization

X-ray diffraction (XRD) was used to identify the particular calcium phosphate phase in the coating. The scans used a 0.02° 2θ step size for 4 s/step over a 30 - 70° 2θ range and a $\text{CrK}\alpha$ radiation source (40 keV, 30 mA). The scans were converted to $\text{CuK}\alpha$ for comparison with the literature. The collected spectra were compared with International Centre for Diffraction Data (ICDD) files.

Scanning Electron Microscopy (SEM) was performed on samples using an accelerating voltage of 30 keV. All samples were cleaned in methanol before sputter coating with gold for analysis. Electron Dispersive Spectroscopy (EDS) was also performed using a 500X scan area and standardless quantification methods using 15 keV accelerating voltage.

Fourier Transform Infrared Spectroscopy (FTIR) was performed in reflectance mode to investigate the surfaces of the samples. This was chosen since the surface of the samples were the focus of the solubility and cell culture studies. The survey was from 0 to 4000 cm^{-1} using 32 scans with 4 cm^{-1} resolution.

Dissolution

A dissolution study was performed based on the procedure by Hyakuna, et al.²⁴ Uncoated and ELD HA coated NPAS and PMOD disks and sintered HA pellets were placed in standard 24-well cell culture dishes and covered with 1 mL of Earle's Balanced Salt Solution (EBSS, part number E3024, Sigma) and placed in an incubator maintained at 37°C and 5% atmospheric CO₂ for up to 14 days. The EBSS was drawn off and replenished with 1 mL of fresh EBSS after time intervals of 0, 1, and 24 h, and at days 2, 3, 5, 7, 10, and 14. At each time period, the removed solute was stored in individual vials and refrigerated. To adjust for evaporation and other possible anomalies, empty wells of the cell culture dishes were used as controls. The 1 mL of solute removed from each sample at each time interval was diluted using 1:21 with deionized distilled water. The diluted samples were analyzed for calcium and phosphorous content using a Perkin Elmer CV-3300 Inductively Coupled Plasma Optic Emission Analysis (ICP). After dissolution studies, the disks were examined using SEM, EDS, FTIR, and XRD.

Cell Culture

Uncoated and ELD HA coated NPAS and PMOD disks were used in cell culture studies. Disks were placed in standard 12-well cell culture plates and sterilized in 70% ethanol for 15 min, then washed with sterilized distilled deionized water three times. Disks from each group were either coated with fetal bovine serum or left uncoated (no serum) and refrigerated in a 4°C coldroom overnight.

Disks were washed three times with phosphate buffered saline (PBS) and seeded with cell suspension. Human MSC, isolated from bone marrow using density gradient centrifugation,²³ were used in all experiments. MSC were obtained with prior approval from the University of Alabama Institutional Review Board, as previously described.²⁵ Cells were detached from tissue culture flasks with 0.05% trypsin/0.1% EDTA solution followed by immediate incubation with trypsin inhibitor. The cells were then washed in serum-free media and seeded on the disks using 1200 microliters of cell suspension containing 1×10^5 MSC in each well. Cells were allowed to attach for either 1 or 24 h in an incubator at 37°C with 5% atmospheric pressure of CO₂.

The disks were then prepared for visualization on a Leitz Orthoplan fluorescent microscope. After incubation, the disks were washed 3 times using PBS, and then covered with 0.1 mL of 3.7% formaldehyde/Tris-buffered saline (TBS) solution for 15 min at room temperature to fix the cells. Disks were then gently washed two times with PBS and incubated for 2 min at room temperature in 0.1 mL of 0.2% TX-100/TBS solution to permeabilize the cells. Disks were again gently washed in PBS twice and blocked 10 min with 0.1 mL of 2% denatured BSA at room temperature. Disks were gently washed twice with PBS, covered with 0.1 mL of Alexa 594-phalloidin (1:200 dilution in TBS), covered in foil, and incubated at 37°C for 1 hour to detect polymerized actin. Disks were washed three times with PBS and hard agitation and then mounted on microscope slides in silicone gaskets (Sigma) with a paraphenylene diamine (Sigma)/glycerol mounting solution and stored at -20°C until observation on the fluorescent microscope.

RESULTS AND DISCUSSION

Coating Fabrication and Characterization

Fabrication was successful in that NPAS and PMOD disks were coated using the ELD system. Characterization led to the conclusion that the deposited coatings were HA. XRD had good agreement with ICDD files for HA and Ti (9-432 and 5-682, respectively). EDS was performed at 15 keV to minimize effects of the underlying titanium substrate on Ca:P quantification. While the ELD HA average Ca:P of 1.55 ± 0.10 was lower than the theoretical 1.67 for HA, it was closer than that found for the sintered HA pellets, 1.30 ± 0.22 . The EDS and XRD concurred that the ELD coatings were HA and comparable to the sintered HA pellets.¹⁷

SEM of the HA ELD coatings revealed well dispersed grains that continuously covered both the NPAS and PMOD surfaces. FTIR of the ELD HA was not consistent with the published data for HA in that the large peak associated with the hydroxyl group at 3570 cm^{-1} was present but not pronounced. The ELD HA and sintered HA pellets were similar in peak number and positions, including the minimized hydroxyl peak. This loss was attributed to the surface roughness of the samples, which most likely scattered the signal during the scans. The agreement of the known hydroxylapatite (sintered HA pellets) spectra with that of the ELD led to the conclusion that it was HA as well.¹⁷

Solubility in EBSS

All of the materials investigated in this study drew calcium and phosphorous from the EBSS solution. This loss from solution indicates that CaP is being deposited on the surfaces of the samples. Figure 2 shows the cumulative Ca and P loss over time. While

there was some inconsistency in the control values, the trend was consistent for the HA ELD disks and the sintered HA pellets. The fact that more Ca and P came out of solution for the sintered HA was not unexpected in that these pellets are porous and have a higher surface area.

SEM of the HA ELD disks revealed some changes to the surfaces. New precipitates were visible on the surface of both the HA NPAS and HA PMOD disks (Figure 3). The presence of the precipitates supports the findings of Ca and P loss from EBSS over the incubation time. EDS reflected a change in the Ca:P ratio for the ELD HA coatings. After 14 days in EBSS the Ca:P ratios decreased (HA NPAS = 1.25 ± 0.17 and HA PMOD = 1.31 ± 0.32 , substrate treatments not statistically different, student t-test $p > 0.05$) compared to ratios before immersion. XRD spectra of the ELD HA had a loss of intensity and some peak broadening. Figure 4 compares representative spectra from samples before and after 14 days in EBSS. There were no new peaks evident after the 14 days in EBSS in the XRD spectra. The data collected from the sintered HA pellet on FTIR after the 14 days was inconclusive, most likely due to the loss of signal by the surface roughness and the difficulty in handling the samples after 14 days in solution. The ELD HA FTIR spectra were not as affected in that there were still comparable peaks with the as-deposited coatings shown in Figure 5. The peak broadening associated with a loss of crystallinity, combined with the lower Ca:P, suggests the new precipitate being a CaP similar to calcium deficient HA.

Cell culture

NPAS and PMOD titanium disks and ELD HA NPAS and PMOD disks were used in the cell culture studies following procedures outlined by Sawyer, et al.²³ All of the disks were either coated with serum or left uncoated prior to seeding with human MSC. As shown in Figure 6, some cells were able to attach to surfaces in the absence of serum pre-coatings, however these cells had a very rounded morphology. In contrast, cells were able to spread on material surfaces that had been pre-coated with serum, suggesting that adsorbed serum proteins play a key role in regulating cell behavior on the ELD HA surfaces. This result is consistent with our prior observation that adsorbed serum factors are required for cell spreading on dense, sintered HA disks.¹¹ At 24 h following seeding, cells on serum coated ELD HA surfaces were better spread and had formed actin stress fibers (Figure 7), a behavior that is favorable for cell survival and osteoblastic differentiation. The observation that cells are able to adhere and spread on serum-coated ELD HA, similar to sintered HA, suggests that the ELD HA coatings would likely be biocompatible in vivo.

CONCLUSIONS

1. ELD coatings were characterized as HA using XRD, EDS, and FTIR elsewhere.¹⁷
2. Neither ELD HA coating lost calcium or phosphorus when exposed to EBSS. ELD HA and sintered HA pellets drew calcium and phosphorous out of EBSS and a secondary phase was visible on the surface of the ELD HA. The resulting phase had a lower Ca:P ratio than HA and was less crystalline.

3. FTIR showed little change in spectra of ELD HA before and after immersion in EBSS for 14 days.
4. Pre-coating the ELD HA samples with serum was required for cell spreading.
5. No differences were noted in the morphology of cells adherent to ELD HA NPAS vs ELD HA NMOD surfaces.

ACKNOWLEDGEMENTS

We would like to thank Mr. Ed Calvert of Wallace State Community College, Hanceville, AL for allowing generous access to the ICP at their facility and Dr. Derrick Dean for providing FTIR data.

REFERENCES

1. Jarcho M. Calcium phosphate ceramics as hard tissue prosthetics. *Clinical Orthopaedics and Related Research* 1981;157:257-278.
2. Cook SD, Thomas KA, Kay JF, Jarcho M. Hydroxyapatite-coated porous titanium for use as an orthopedic biologic attachment system. *Clinical Orthopaedics and Related Research* 1988;230:303-312.
3. Cook SD, Thomas KA, Dalton JF, Volkman TK, Whitecloud TS, Kay JF. Hydroxylapatite coatings of porous implants improves bone ingrowth and interface attachment strength. *Journal of Biomedical Materials Research* 1992;26:989-1001.
4. Morris HF, Ochi S. Hydroxyapatite-coated implants: a case for their use. *Journal of Oral and Maxillofacial Surgery* 1998;56(11):1303-1311.
5. Bagambisa FB, Joos U, Schilli W. Mechanisms and structure of the bond between bone and hydroxyapatite. *Journal of Biomedical Materials Research* 1993;27:1047-1055.

6. Hench LL. Ceramics, glasses, and glass-ceramics. In: Ratner BD, Hoffman AS, Schoen FJ, Lemons JE, editors. *Biomaterials science: an introduction to materials in medicine*. San Diego: Academic Press; 1996. p 73-84.
7. Johnsson MS, Nancollas GH. The role of brushite and octacalcium phosphate in apatite formation. *Critical Reviews in Oral Biology and Medicine* 1992;3(1-2):61-82.
8. Daculsi G, LeGeros RZ, Nery E, Lynch K, Kerebel B. Transformation of biphasic calcium phosphate ceramics *in vivo*: ultrastructural and physicochemical characterization. *Journal of Biomedical Materials Research* 1989;23(8):883-894.
9. LeGeros RZ. *Calcium phosphates in oral biology and medicine*. San Francisco: Karger; 1991.
10. Horbett TA. Proteins: structure, properties, and adsorption. In: Ratner BD, Hoffman AS, Schoen FJ, Lemons JE, editors. *Biomaterials science: an introduction to materials in medicine*. San Diego: Academic Press; 1996. p 133-141.
11. Kilpadi KL, Chang PL, Bellis SL. Hydroxylapatite binds more serum proteins, purified integrins, and osteoblast precursor cells than titanium or steel. *Journal of Biomedical Materials Research* 2001;57(2):258-267.
12. Ducheyne P, Qiu Q. Bioactive ceramics: the effect of surface reactivity on bone formation and bone cell function. *Biomaterials* 1999;20(11):2287-2303.
13. Zeng H, Chittur KK, Lacefield WR. Analysis of bovine serum albumin adsorption on calcium phosphate and titanium surfaces. *Biomaterials* 1999;20:377-384.
14. ter Brugge PJ, Wolke JG, Jansen JA. Effect of calcium phosphate coating crystallinity and implant surface roughness on differentiation of rat bone marrow cells. *Journal of Biomedical Materials Research* 2002;60(1):70-78.
15. Globus RK, Doty SB, Lull JC, Holmuhamedov E, Humphries MJ, Damsky CH. Fibronectin is a survival factor for differentiated osteoblasts. *Journal of Cell Science* 1998;111:1358-1393.
16. Otto WR, Rao J. Tomorrow's skeleton staff: mesenchymal stem cells and the repair of bone and cartilage. *Cell Proliferation* 2004;37:97-110.

17. Davis RSOC, Venugopalan R, Bellis SL, Janowski GM. Electrolytic deposition of hydroxylapatite using a pulsed wave technique. Unpublished data 2005.
18. Shirkhanzadeh M. Hydroxyapatite particles prepared by electrocrystallization from aqueous electrolytes. *Materials Letters* 1993;15(5-6):392-395.
19. Shirkhanzadeh M. Direct formation of nanophase hydroxyapatite on cathodically polarized electrodes. *Journal of Materials Science: Materials in Medicine* 1998;9:67-72.
20. Yen SK, Lin CM. Cathodic reactions of electrolytic hydroxyapatite coating on pure titanium. *Materials Chemistry and Physics* 2002;77:70-76.
21. Becker P, Neumann H-G, Nebe B, Luthen F, Rychly J. Cellular investigations on electrochemically deposited calcium phosphate composites. *Journal of Materials Science: Materials in Medicine* 2004;15:437-440.
22. Ban S, Maruno S, Arimoto N, Harada A, Hasegawa J. Effect of electrochemically deposited apatite coating on bonding of bone to the HA-G-Ti composite and titanium. *Journal of Biomedical Materials Research* 1997;36:9-15.
23. Sawyer AA, Hennessy KM, Bellis SL. Regulation of mesenchymal stem cell attachment and spreading on hydroxyapatite by RGD peptides and adsorbed serum proteins. *Biomaterials* 2005;26:1467-1475.
24. Hyakuna K, Yamamuro T, Kotoura Y, Oka M, Nakamura T, Kitsugi T, Kokubo T, Kushitani H. Surface reactions of calcium phosphate ceramics to various solutions. *Journal of Biomedical Materials Research* 1990;24(4):471-488.
25. Kilpadi KL, Sawyer AA, Prince CW, Chang P-L, Bellis SL. Primary human marrow stromal cells and Saos-2 osteosarcoma cells use different mechanisms to adhere to hydroxylapatite. *Journal of Biomedical Materials Research* 2004;68A(2):273-285.

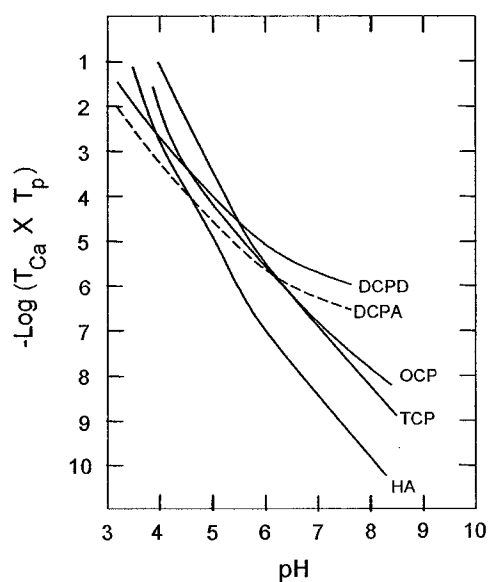


Figure 1. Schematic of solubility isotherms of CaP phases at 37°C and 0.10 M ionic activity. Republished with the permission of the International and American Associations for Dental Research, from Johansson⁷; permission conveyed through Copyright Clearance Center, Inc.

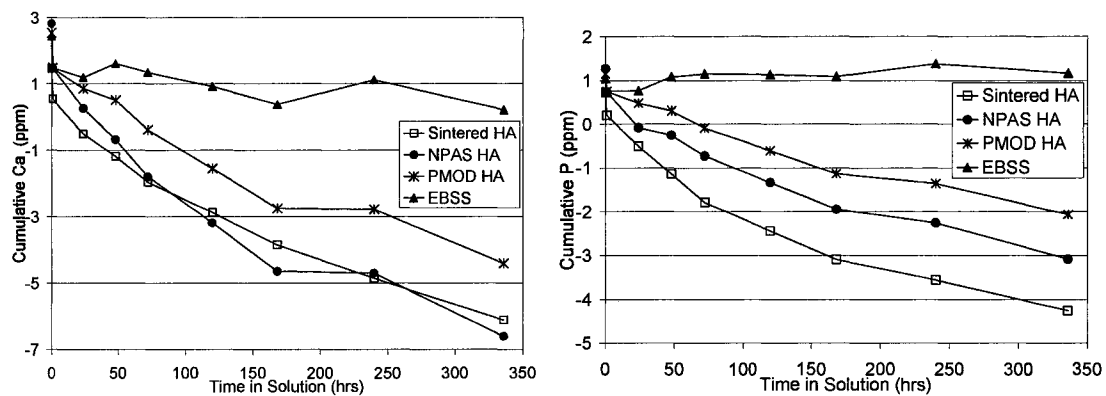


Figure 2. ICP Cumulative graphs of Ca and P coming out of solution and onto HA surfaces over a 14 day period.

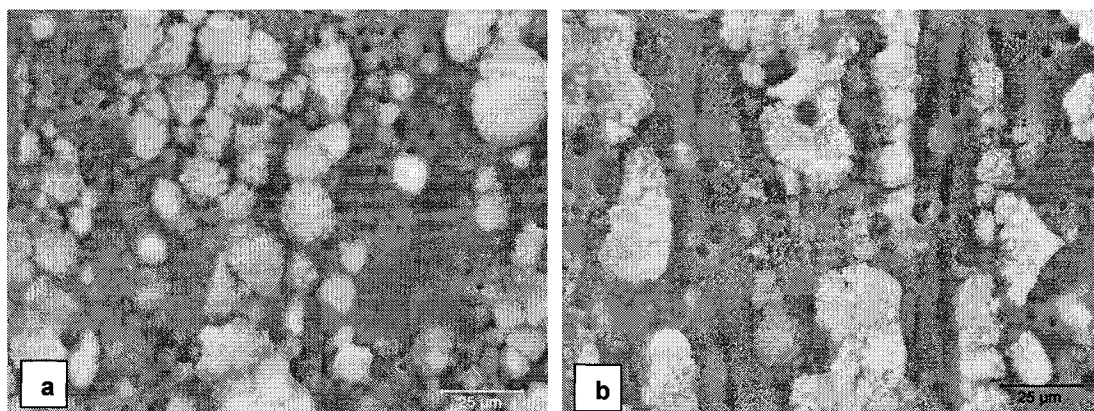


Figure 3. SEM images of ELD HA before (a) and after 14 days in EBSS (b).

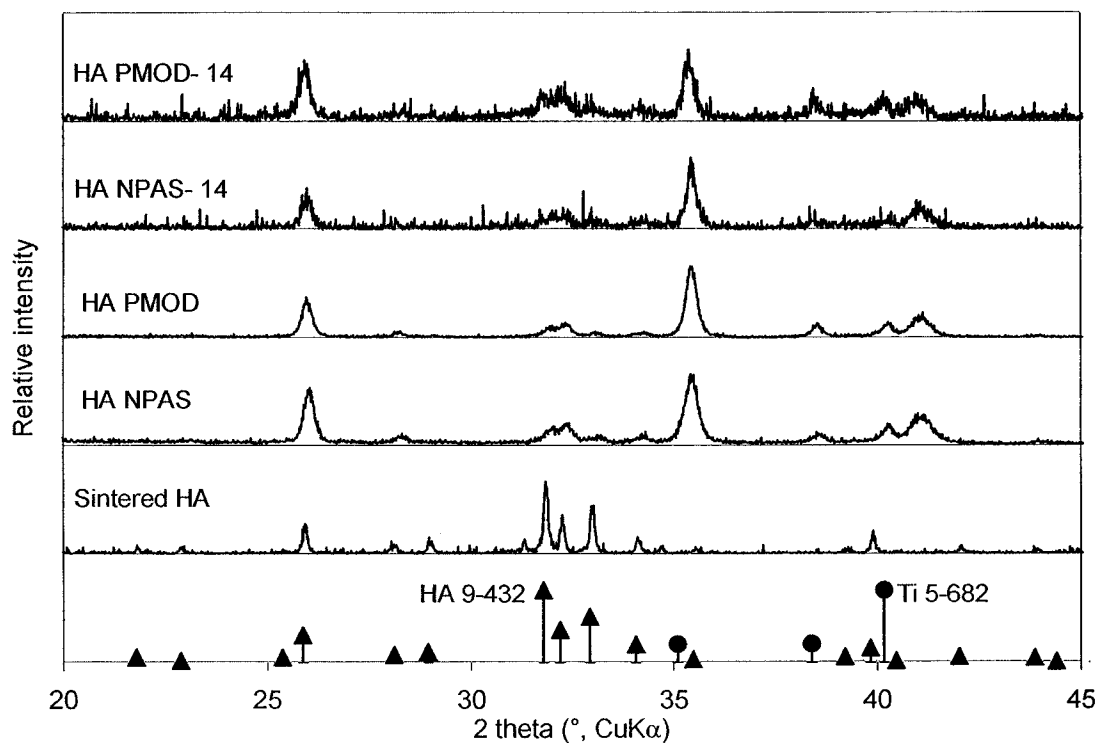


Figure 4. Representative XRD spectra of samples before (HA PMOD and HA NPAS) and after dissolution (HA PMOD-14 and HA NPAS-14) compared to ICDD files for HA (9-432) and titanium (5-682).

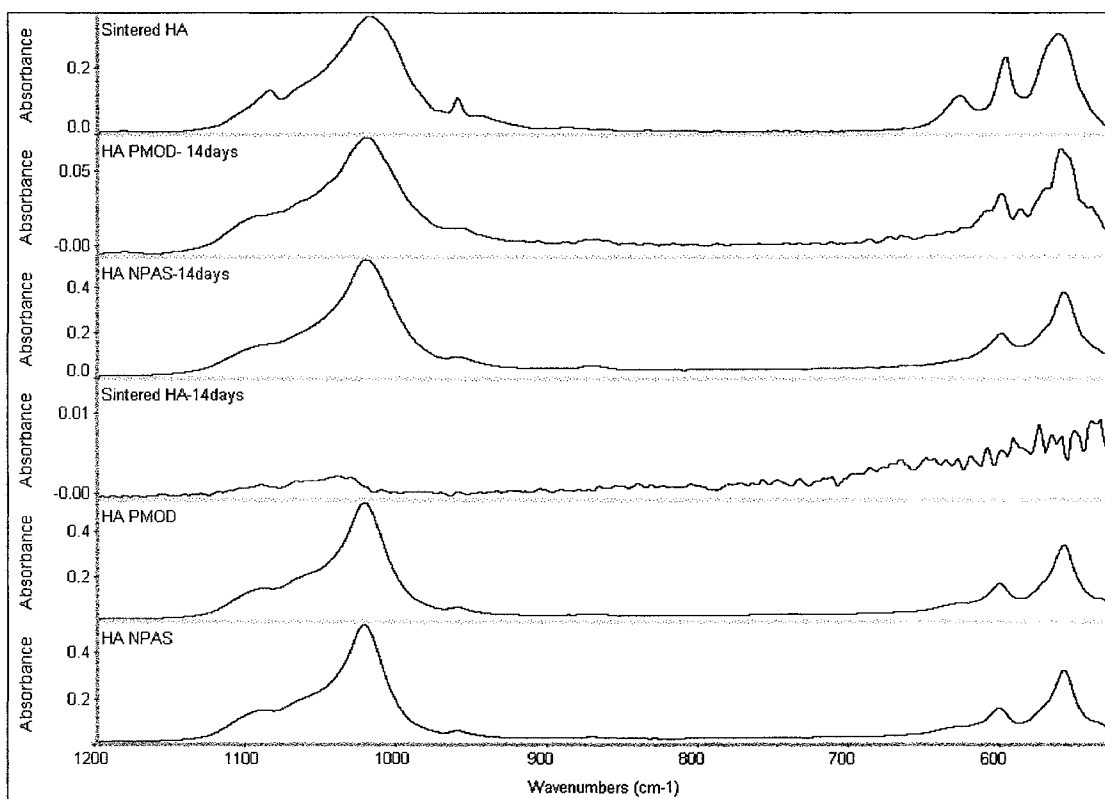


Figure 5. FTIR spectra of samples before and after 14 day solubility study in EBSS.



Figure 6. MSC on surfaces after 1 h of incubation. Surfaces were either coated with serum or left uncoated before cell seeding. Serum was required for cells to spread on all surfaces.

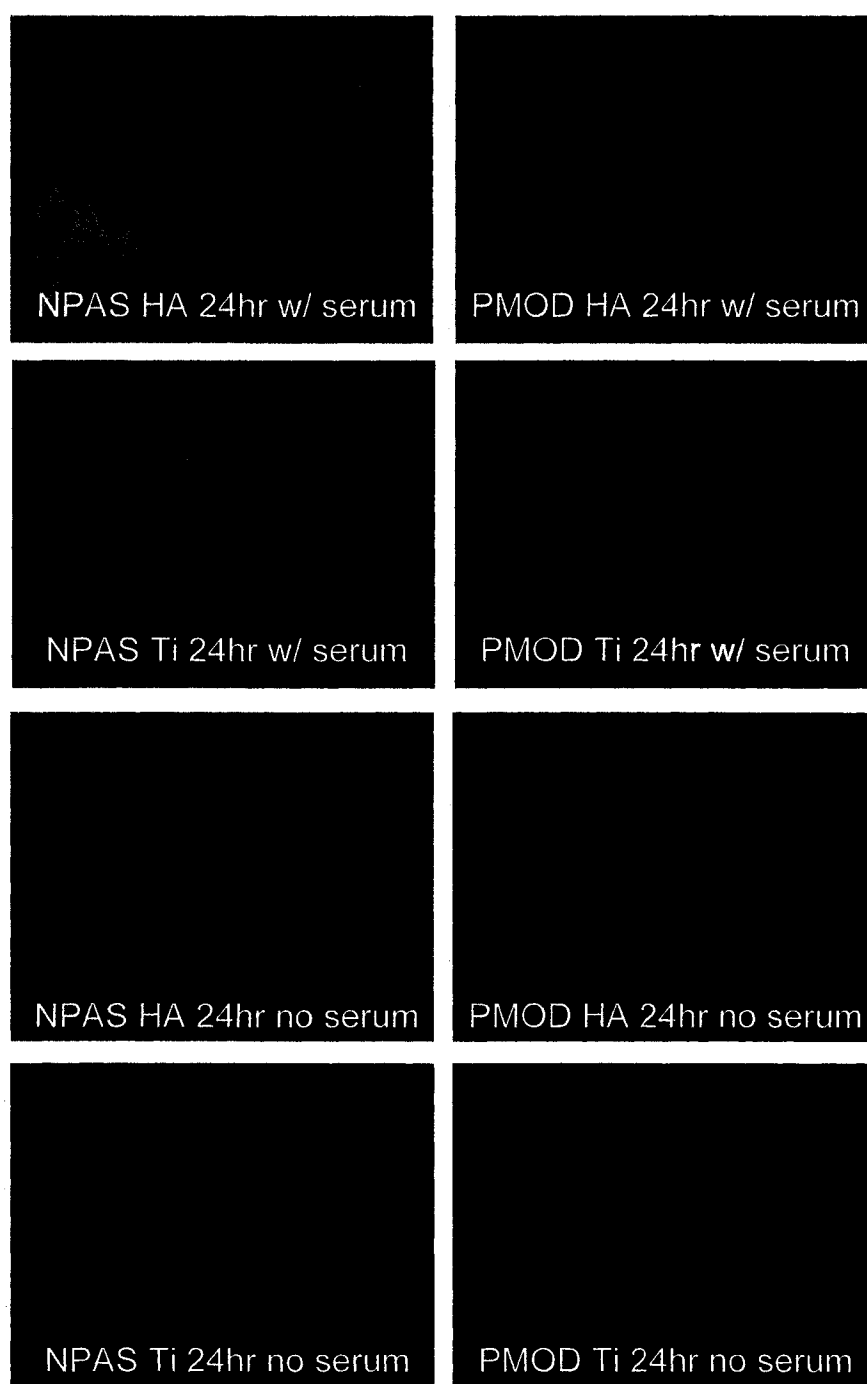


Figure 7. MSC on surfaces after 24 h incubation. Stress fibers are visible at this time period on ELD HA surfaces coated with serum while cells on ELD HA surfaces not coated with serum were rounded. Interestingly, in contrast to ELD HA coated materials, uncoated NPAS and PMOD Ti surfaces were able to promote spreading in the absence of adsorbed serum factors.

OVERALL RESULTS AND DISCUSSION

From the findings of the three preceding manuscripts, it can be concluded that a reproducible low temperature process has been developed using simple chemistry to deposit both resorbable and nonresorbable biocompatible coatings having potential for development into biomedical applications. However, the manuscript format merits a single discussion to better emphasize the conceptual commonalities among these papers.

Substrate Treatment Effects

The substrate surfaces were given either nitric acid passivation (NPAS) or phosphoric acid pickling (PMOD). The surfaces of the two treatments were morphologically identical, but chemically different. XPS detected phosphorus only on the uncoated PMOD surface; this difference was not detected using EDS. After coating with calcium phosphate (CaP) using electrolytic deposition (ELD), substrates were placed in an ultrasonic bath of methanol for 2 min. The ELD coatings were still present on the both substrate treatments, but SEM showed that more nucleation sites and better crystal definition occurred on the PMOD compared to the NPAS for both the resorbable and nonresorbable CaP (Figure 1). A dispersion of nucleation sites is beneficial in providing continuous coatings on complex geometries and enhances the ease with which this technique can be applied.⁴⁴ The augmented nucleation on the PMOD surface may be due to the phosphorous on the substrate. The fact that more coating remained on the PMOD surface after

sonication may be a result of phosphorous either creating more nucleation sites, enhancing the chemical bond of CaP to the substrate, or a combination of the two.

These substrate treatment differences were no longer evident once the coatings attained complete coverage. The deposited coatings were indistinguishable by substrate treatment using XRD, XPS, SEM, EDS, and FTIR. Both treatments had high bond strengths for deposited coatings, values 2 to 60 times other published values, approaching the limit for the strength of the epoxy used for testing (70 MPa). The combination of the high measured strengths with the behavior in the ultrasonic bath led to the qualitative assessment that the ELD CaP coatings investigated were well bonded to the Ti surfaces regardless of substrate treatment.

Electrolytic Deposition Coating Method

A repeatable process was developed using ELD to coat CaP on Ti substrates. XRD, XPS, SEM and EDS and FTIR revealed consistent spectra and morphology for the coatings deposited using like conditions.

Resorbable Calcium Phosphate Coatings

Constant current electrolytic deposition in an acidic starting solution deposited a resorbable CaP coating composed of predominantly octacalcium phosphate (OCP) and hydroxylapatite (HA), as predicted by solubility isotherms for CaP.^{15,18} XRD spectra were in good agreement with the ICDD files 26-1056 for OCP and 9-432 for HA. EDS values for the Ca to P ratio were between the stoichiometric values for OCP and HA, 1.33

and 1.67, respectively (NPAS = 1.46 ± 0.02 , PMOD = 1.46 ± 0.03), further supporting the presence of the two CaP phases.

The pH and pH changes are critical to the ELD process. The starting pH of the CaP electrolyte was 4.0 ± 0.1 which changed to 7.5 ± 0.1 at the end of the deposition. The low pH favors the electro-reduction reaction of $2\text{H}^+ + 2\text{e}^- \rightarrow \text{H}_2$ due to the high activity of the hydrogen ions.⁴⁹ This reaction has two key effects as hydrogen ions are consumed: hydrogen gas is evolved, and the pH is increased at the cathode. The pH at the cathode controls the CaP deposition process and gradually increases the bath pH. As described earlier in the introduction of the dissertation, HA becomes the stable CaP phase as pH increases, illustrated in the solubility isotherms in Figure 2.^{15,18} Because the solution was not buffered, the higher localized substrate pH increased overall pH in the bulk solution as well. As the pH increases, the H^+ activity decreases,⁴⁹ and the dominant reaction at the cathode becomes reduction of water molecules to hydrogen gas and hydroxyl groups.⁴⁹⁻⁵¹ These hydroxyl groups in turn can become involved in reactions at the cathode.⁴⁹⁻⁵¹ Some example reactions for electrochemical system using CaP electrolyte and Ti cathode are listed in Table 1.

TABLE 1. Reactions involving hydroxyl groups at the Ti cathode in a CaP electrolyte.

With the acid phosphates in the solution:	$\text{HPO}_4^{2-} + (\text{OH})^- \rightarrow \text{H}_2\text{O} + \text{PO}_4^{3-}$
With the substrate surface:	$\text{TiO}_2 + 2 \text{H}_2\text{O} + \text{e}^- \rightarrow \text{Ti}(\text{OH})^3 + (\text{OH})^-$
With the CaP ions in solution:	$10\text{Ca}^{2+} + 6\text{PO}_4^{3-} + 2(\text{OH})^- \rightarrow \text{Ca}_{10}(\text{PO}_4)_6(\text{OH})_2$

The increase in pH within the diffusion layer at the cathode permits the formation of stable CaP coatings from unsaturated solutions. The Gibbs free energy was calculated

for CaP using the starting bath conditions for the electrolyte used to deposit resorbable CaP.⁷³ The electrolyte was not saturated to form any phase of CaP at the initial pH or molar concentration. The change in the total CaP molar concentrations of the electrolyte at the end of deposition was negligible, enabling comparison of the pH versus Gibbs free energy. This is due to the large electrolyte volume relative to the coating amount. The plot of the Gibbs free energy of the starting molar concentrations at various pH values in Figure 3 shows that for the deposition of OCP and HA to occur, pH must increase, acting as the driving force for deposition and supporting the occurrence of the reactions described above.

Nonresorbable Calcium Phosphate Coatings

The bath chemistry was altered by increasing the Ca to P molar ratio (Ca:P) to 1.67 and having a neutral starting pH to deposit a nonresorbable CaP. Using the same constant current techniques employed previously produced discontinuous coatings and resulted in precipitate formation in the bath.

Application of a pulsed wave is often used in electroplating to improve dispersion of the deposited materials.⁷⁴ Using a symmetric square wave, pulsed deposition in the neutral CaP electrolyte produced continuous nonresorbable CaP coatings consisting predominantly of HA. The starting pH of the solution was 6.1 ± 0.1 and increased to 6.9 ± 0.1 after deposition. due to the higher pH at the start, the HPO_4^{2-} ions are converted to PO_4^{3-} , providing the ions for the reactions described in Table 1.⁴⁹⁻⁵¹

The “off period” of the pulse allowed the slower, larger PO_4^{3-} ions to catch up with the faster, smaller Ca^{2+} ions at the cathode surface⁷⁵ as well as to relax the diffusion

layer and the associated pH and concentration gradients⁴⁹ (Figure 4). This relaxation allows the cathode pH and ionic concentrations to approach those of the bulk electrolyte.^{44,76} This also explains why this system was unable to deposit a continuous HA coating using the constant current. The increase in pH during constant current deposition was so great that no CaP phase was stable. Again, the change in molar concentration of the CaP electrolyte was negligible after coating deposition. Plotting the Gibbs free energy as a function of pH at the initial Ca and P molar concentrations in Figure 5 shows that as the pH increases there are no stable phases of CaP. During constant current deposition, the optimal pH for HA deposition was reached in the diffusion layer, not at the cathode surface, causing precipitates to form in the diffusion layer and not on the surface.

XRD spectra were found to match with ICDD files 9-432 for HA and 5-682 for Ti and indicate the possibility of another CaP phase with a peak around 42° 2 theta $\text{CuK}\alpha$, which did not match known CaP phases. EDS supported the finding of a CaP that was mostly HA having Ca to P ratio of 1.55 ± 0.10 for the ELD coatings, consistent with a calcium deficient apatite. Commercially available HA powder (Fisher) was pressed into pellets and used for comparison to the ELD HA coatings. These pellets were found to be similar using XRD, EDS, and FTIR, further evidence that the nonresorbable ELD coatings were HA.

Solubility in Earle's Balanced Salt Solution

The resorbable ELD CaP released Ca and P into the Earle's Balanced Salt Solution (EBSS) over the 14 day incubation period. Coating loss was visible, and a change in the Ca:P occurred. The release of the Ca and P can be explained by the solubility iso-

therm in Figure 2. While HA and OCP occur below the line for the EBSS concentration, indicating that they are stable in the environment, the likely presence of a metastable CaP would allow for the dissolution of the coating into the EBSS. The data collected using Inductively Coupled Plasma Spectroscopy indicated that, after the initial release of Ca and P into solution, a plateau was reached indicative of a probable dynamic equilibrium.

The nonresorbable ELD HA coating did not release Ca or P into the EBSS. Instead Ca and P were drawn out of solution and deposited on the ELD coatings, as well as on to the HA pellets used for comparison. Again referring to Figure 2, HA is thermodynamically stable in EBSS and can act as a seed site for CaP to form from solution.¹⁸ There were visible changes in the ELD HA coating morphology. This change also decreased the crystallinity and weakened the ELD HA coating. XRD showed broadening of the peaks, indicative of lower crystallinity. The bond strength did decrease for the coating post dissolution, but after 14 days, the bond strength was still comparable to, or exceeded, other published values (NPAS = 44 ± 21 MPa, PMOD = 38 ± 7 MPa). The comparable behavior of the ELD HA and HA pellets is encouraging for the use of ELD HA as a biocompatible material.

Cell Culture

Human mesenchymal stem cells (MSC) spread on both the ELD HA and uncoated substrates in the presence of serum, regardless of substrate treatment; no cell spreading occurred on the surfaces without serum. MSC behavior on the ELD HA surfaces was comparable to that on the Ti. Cell spreading was seen in the first hour of incubation while cytoskeleton and stress fibers developed by the 24 h period. This behavior is similar to

that seen in previous work using the same type of HA pellets that were used in this study as characterization comparisons. The HA pellets were found to adsorb more adhesion proteins, and, in turn bound more fibronectin, vitronectin, and osteoblast precursor cells than metals.⁷² The similarities between the ELD HA and HA pellets in terms of material characterization, behavior in biological saline, and behavior with MSC suggest that the ELD HA may show such favorable cell binding as well.

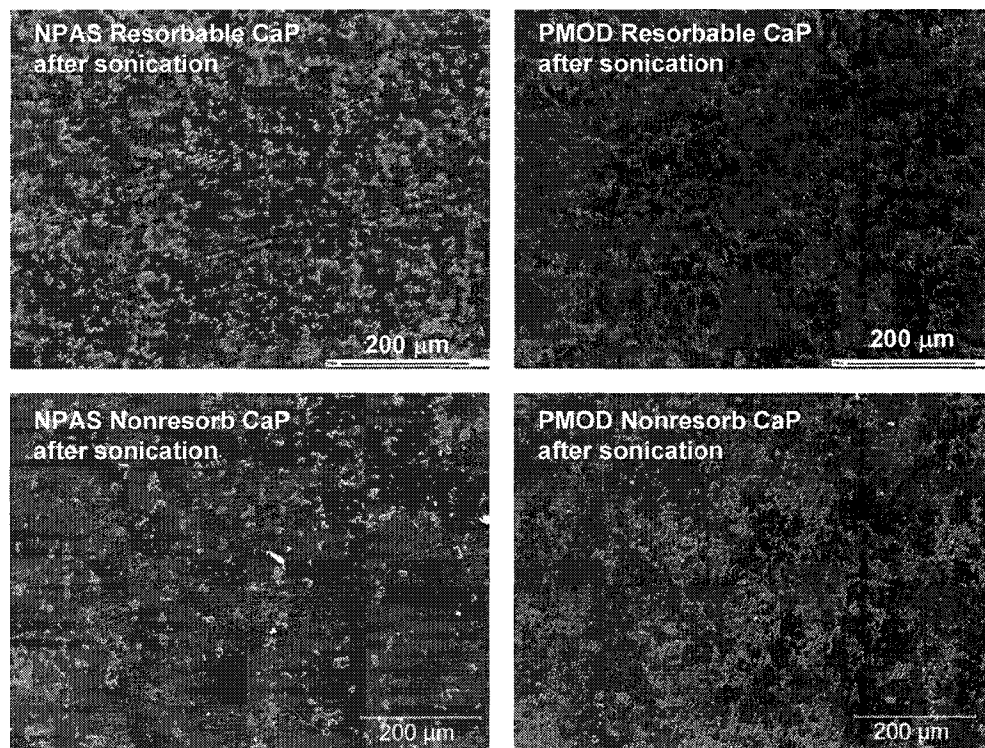


Figure 1. ELD coated surfaces after 2 minutes in ultrasonic bath of methanol. Coatings are still present on the Ti, but there are more nucleation sites on the PMOD surfaces.

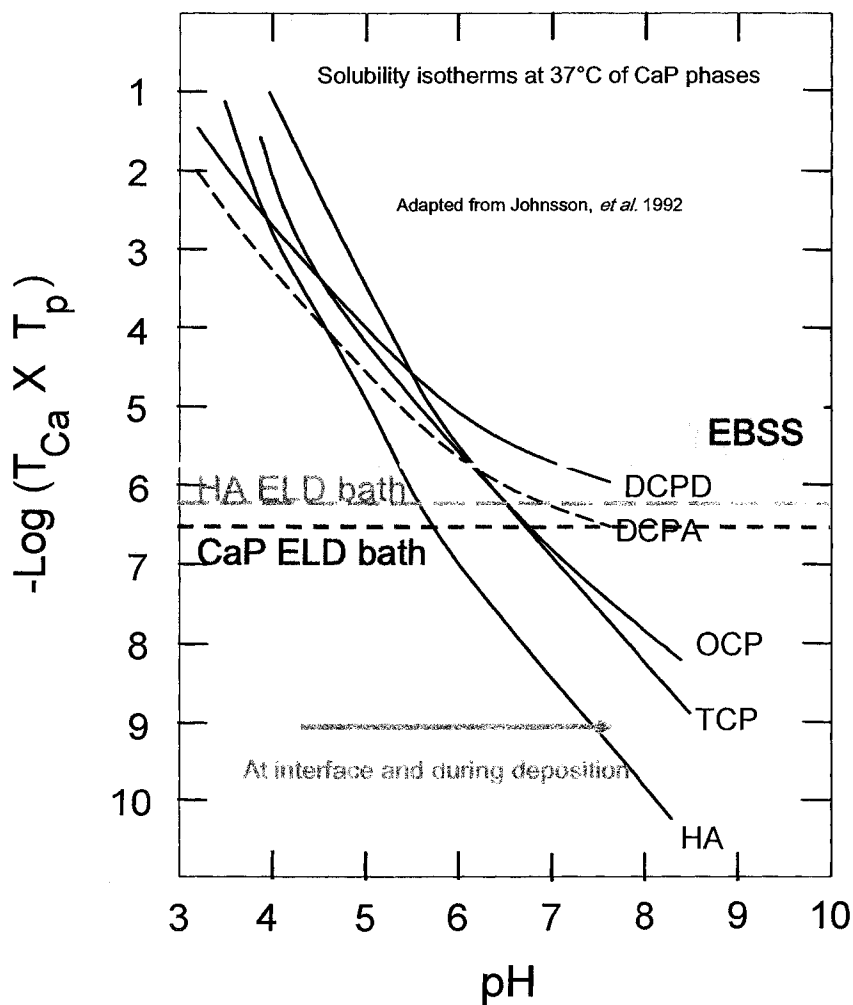


Figure 2. CaP solubility isotherms as applied to the systems used in this study. Negative log of the product of total molar calcium and phosphorous content plotted versus pH. Adapted from Johnsson.¹⁸ Republished with the permission of the International and American Associations for Dental Research; permission conveyed through Copyright Clearance Center, Inc.

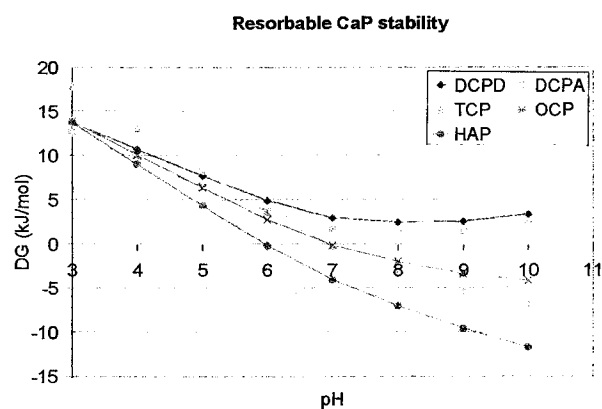


Figure 3. Phase stability of the resorbable CaP electrolyte system (Ca and P molar concentrations held constant, equal to 6.1×10^{-4} M).

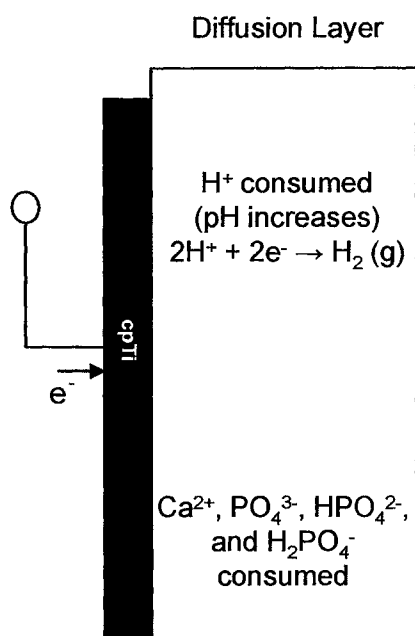
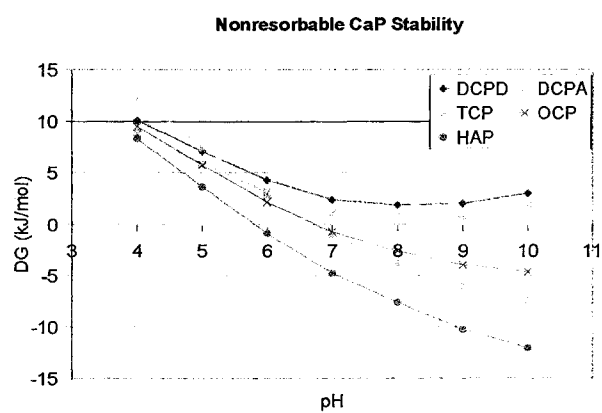


Figure 4. Schematic representing the reactions at the cathode surface during ELD of CaP.



Figures 5. Phase stability of the nonresorbable CaP electrolyte system (Ca and P molar concentrations held constant, $[Ca] = 1.0 \times 10^{-4} \text{ M}$, $[P] = 6.0 \times 10^{-4} \text{ M}$).

CONCLUSIONS

The specific aims for this research were met. In detail:

1. *Electrodeposit a resorbable calcium phosphate coating on modified titanium substrates using constant current techniques and an unbuffered electrolyte.*
 - a. *Fabricate a CaP coating on Ti substrates with either NPAS or PMOD treatment.*
 - b. *Ascertain crystal structure and coverage.*
 - c. *Measure bond strength.*
 - d. *Quantify the amounts of elements released from coating in a biological saline.*
- A repeatable ELD process was developed to deposit a resorbable CaP that was predominantly composed of octacalcium phosphate (OCP) and hydroxylapatite (HA). Although substrate treatment apparently affected the nucleation density, no other effects on coating behavior were observed. Bond strengths for the ELD coatings were equal to, or exceeded, maximum values measurable with this method (69 MPa); this data in combination with coating presence after placement in an ultrasonic bath led to the qualitative assessment that coating bonded well to the substrates. Ca and P were released when placed in a biological saline.
2. *Electrodeposit a nonresorbable coating on modified titanium substrates in an unbuffered CaP electrolyte.*

- a. Fabricate a hydroxylapatite coating on Ti substrates with either NPAS or PMOD treatment.*
- b. Ascertain crystal structure and coverage.*
- c. Measure bond strength.*

HA coatings were deposited using ELD by changing the starting pH, Ca to P ratio, and applied current. Due to pH and transport effects at the interface, it was necessary to use a square wave, rather than a constant current for deposition. Again, substrate treatment apparently affected the nucleation density, but did not alter any other coating behavior. The ELD HA coatings were similar to bulk HA pellets using the characterization techniques of this study. Measured bond strengths for the ELD HA coating exceeded most published values that used similar testing methods. This data, in combination with the presence of the coating after ultrasonication, characterized the coatings as having good bond strengths.

- 3. *Determine biocompatibility of ELD HA coated samples compared to uncoated Ti substrates and sintered HA pellets.*
 - a. Quantitatively compare the elements released by ELD HA and Ti to those released by sintered HA pellets in a biological saline.*
 - b. Characterize the properties of the surfaces post exposure to biological saline solution.*
 - c. Compare the cell morphology of osteoprogenitor cells on the different surfaces.*

It was found that the ELD HA was comparable to bulk HA pellets in terms of dissolution behavior (i.e., additional CaP deposited from the biological saline with a less

crystalline structure). ELD HA had similar results when exposed to MSC, as did HAS in earlier studies.

4. *Demonstrate control of the electrolytic deposition system to deposit desired CaP coating*
 - a. *Develop an understanding of the electrolytic deposition of CaP using an unbuffered CaP containing electrolyte*
 - b. *Determine effects of adjusting pH, ion concentration, and applied current density on CaP deposition*
 - c. *Utilize thermodynamics, kinetics, and deposition parameters to optimize interface chemistry for desired CaP deposition*

An understanding has been developed of the ELD system with this electrolyte through the use of solubility isotherms and Gibb's free energy plots. The roles of pH, deposition current, and constant current/pulsed current were addressed.

FUTURE WORK

Deposition of calcium phosphates using electrolytic deposition shows much promise for further research and clinical application. Several aspects merit further investigation:

- Measure bond strength of the coating to the substrate using other techniques.
There are other standard bond strength methods used by industry for biomedical implant coatings.
- Further optimize the pulsed deposition using the Gibb's free energy of the system and transport analysis.
- Explore the possibility of deposition on more complex geometries as well as scaling the system up to deposit coatings on larger surface areas.
- Further compare the cellular behavior of the ELD HA compared to bulk HA, which is one more step toward establishing ELD calcium phosphate coatings as biocompatible materials.

LIST OF GENERAL REFERENCES

1. Schneider SJ. Engineered Materials Handbook: Vol. 4-Ceramics and Glasses. In: ASM, editor. Engineered Materials Handbook. USA: ASM International; 1991. p 1007-1013.
2. Park J, Lakes RS. Biomaterials: an introduction. New York: Plenum Press; 1992.
3. Knowles JC, Gross K, Berndt CC, Bonfield W. Structural changes of thermally sprayed hydroxyapatite investigated by Rietveld analysis. Biomaterials 1996;17(6):639-645.
4. Ratner BD, Hoffman AS, Schoen FJ, Lemons JE, editors. Biomaterials science: an introduction to materials in medicine. San Diego: Academic Press; 1996.
5. Soballe K, Toksvig-Larsen S, Gelineck J, Fruensgaard S, Hansen ES, Ryd L, Lucht U, Bunger C. Migration of hydroxyapatite coated femoral prostheses. A Roentgen Stereophotogrammetric study. Journal of Bone and Joint Surgery. British Volume 1993;75(5):681-687.
6. Jarcho M. Calcium phosphate ceramics as hard tissue prosthetics. Clinical Orthopaedics and Related Research 1981;157:257-278.
7. Ducheyne P, Hench LL, Kagan A, Martens M, Burssens A, Mulier JC. The effect of hydroxyapatite impregnation on skeletal bonding of porous coated implants. Journal of Biomedical Materials Research 1980;14:225-237.
8. Cook SD, Thomas KA, Kay JF, Jarcho M. Hydroxyapatite-coated porous titanium for use as an orthopedic biologic attachment system. Clinical Orthopaedics and Related Research 1988;230:303-312.
9. Rivero DP, Fox J, Skipor AK, Urban RM, Galante JO. Calcium phosphate-coated porous titanium implants for enhanced skeletal fixation. Journal of Biomedical Materials Research 1988;22:191-202.

10. Filiaggi MJ, Pilliar RM, Abdulla D. Evaluating sol-gel ceramic thin films for metal implant applications. II. Adhesion and fatigue properties of zirconia films on Ti-6Al-4V. *Journal of Biomedical Materials Research* 1996;33(4):225-238.
11. Hayakawa T, Yoshinari M, Nemoto K, Wolke JG, Jansen JA. Effect of surface roughness and calcium phosphate coating on the implant/bone response. *Clinical Oral Implants Research* 2000;11(4):296-304.
12. Daculsi G, LeGeros RZ, Nery E, Lynch K, Kerebel B. Transformation of biphasic calcium phosphate ceramics *in vivo*: ultrastructural and physicochemical characterization. *Journal of Biomedical Materials Research* 1989;23(8):883-894.
13. Ducheyne P, Radin S, King L. The effect of calcium phosphate ceramic composition and structure on *in vitro* behavior. I. Dissolution. *Journal of Biomedical Materials Research* 1993;27:25-34.
14. Overgaard S, Lind M, Glerup H, Grundvig S, Bunger C, Soballe K. Hydroxyapatite and fluorapatite coatings for fixation of weight loaded implants. *Clinical Orthopaedics and Related Research* 1997;336:286-296.
15. Brown WE, Chow LC, inventor; American Dental Association Health Foundation, assignee. Dental restorative cement pastes. United States patent 4518430. 1985 May 21.
16. Nancollas GH. Physical chemistry of crystal nucleation growth and dissolution of stones. In: Wickham JEA, Buck AC, editors. *Renal tract stones: metabolic basis and clinical practice*. London: Churchill Livingstone; 1989.
17. Brown WE. Crystal structure of octacalcium phosphate. *Nature* 1962;196:1048-1050.
18. Johnsson MS, Nancollas GH. The role of brushite and octacalcium phosphate in apatite formation. *Critical Reviews in Oral Biology and Medicine* 1992;3(1-2):61-82.
19. LeGeros RZ. *Calcium phosphates in oral biology and medicine*. San Francisco: Karger; 1991.

20. Kumar M, Xie J, Chittur K, Riley C. Transformation of modified brushite to hydroxyapatite in aqueous solution: effects of potassium substitution. *Biomaterials* 1999;20(15):1389-1399.
21. LeGeros RZ, Daculsi G. *In vivo* transformation of biphasic calcium phosphate ceramics: ultrastructural and physicochemical characterizations. In: Yamamuro T, Hench LL, Wilson J, editors. *CRC Handbook of bioactive ceramics*. Boca Raton: CRC Press, Inc.; 1990. p 17-28.
22. Nancollas GH. The involvement of calcium phosphates in biological mineralization and demineralization processes. *Pure and Applied Chemistry* 1992;64(11):1673-1678.
23. Hench LL. Ceramics, glasses, and glass-ceramics. In: Ratner BD, Hoffman AS, Schoen FJ, Lemons JE, editors. *Biomaterials science: an introduction to materials in medicine*. San Diego: Academic Press; 1996. p 73-84.
24. de Groot K, Klein CPAT, Wolke JGC, de Blieck-Hogervorst JMA. Chemistry of calcium phosphate bioceramics. In: Yamamuro T, Hench LL, Wilson J, editors. *CRC Handbook of bioactive ceramics*. Boca Raton: CRC Press, Inc.; 1990. p 3-16.
25. Dalton JE, Cook SD. *In vivo* mechanical and histological characteristics of HA-coated implants vary with coating vendor. *Journal of Biomedical Materials Research* 1995;29:239-245.
26. McPherson R, Gane N, Bastow TJ. Structural characterization of plasma-sprayed hydroxylapatite coatings. *Journal of Materials Science: Materials in Medicine* 1995;6:327-334.
27. Tong W, Chen J, Zhang X. Amorphization and recrystallization during plasma spraying of hydroxyapatite. *Biomaterials* 1995;16(11):829-832.
28. Vogel J, Russel C, Gunther G, Hartmann P, Vizethum F, Bergner N. Characterization of plasma-sprayed hydroxyapatite by ³¹P-MAS-NMR and the effect of subsequent annealing. *Journal of Materials Science: Materials in Medicine* 1996;7:495-499.
29. Albrektsson T. Hydroxyapatite-coated implants: a case against their use. *Journal of Oral and Maxillofacial Surgery* 1998;56(11):1312-1326.

30. Lucas LC, Lacefield WR, Ong JL, Whitehead RY. Calcium phosphate coatings for medical and dental implants. *Colloids and Surfaces A: Physicochemical and Engineering Aspects* 1993;77:141-147.
31. Ji H, Marquis PM. Effect of heat treatment on the microstructure of plasma-sprayed hydroxyapatite coating. *Biomaterials* 1993;14(1):64-68.
32. Wie H, Hero H, Solheim T, Kleven E, Rorvik AM, Haanaes HR. Bonding capacity in bone of HIP-processed HA-coated titanium: mechanical and histological investigations. *Journal of Biomedical Materials Research* 1995;29(11):1443-1449.
33. Han Y, Xu K, Lu J. Dissolution response of hydroxyapatite coatings to residual stresses. *Journal of Biomedical Materials Research* 2001;55(4):596-602.
34. Zyman Z, Weng J, Liu X, Li X, Zhang X. Phase and structural changes in hydroxyapatite coatings under heat treatment. *Biomaterials* 1994;15(2):151-155.
35. Wang BC, Chang E, Lee TM, Yang CY. Changes in phases and crystallinity of plasma-sprayed hydroxyapatite coatings under heat treatment: A quantitative study. *Journal of Biomedical Materials Research* 1995;29:1483-1492.
36. Ong JL, Lucas LC, Lacefield WR, Rigney ED. Structure, solubility and bond strength of thin calcium phosphate coatings produced by ion beam sputter deposition. *Biomaterials* 1992;13:249-254.
37. Jansen JA, Wolke JG, Swann S, van der Waerden JP, de Groot K. Application of magnetron sputtering for producing ceramic coatings on implant materials. *Clinical Oral Implants Research* 1993;4:28-34.
38. Ong JL, Lucas LC. Post-deposition heat treatments for ion beam sputter deposited calcium phosphate coatings. *Biomaterials* 1994;15:337-341.
39. Rigney E. Characterization of ion-beam sputter deposited Ca-P films [Dissertation]. Birmingham, AL: University of Alabama at Birmingham; 1989.
40. Zeng H. Evaluation of bioceramic coatings produced by pulsed laser deposition and ion beam sputtering [Dissertation]. Birmingham, AL: University of Alabama at Birmingham; 1997.

41. Wen HB, Wolke JG, de Wijn JR, Liu Q, Cui FZ, de Groot K. Fast precipitation of calcium phosphate layers on titanium induced by simple chemical treatments. *Biomaterials* 1997;18(22):1471-1478.
42. Li P, Matthews F. The solution-induced three-dimensional transformation of porous titanium ingrowth surfaces into a carbonated apatite for enhancing bone ingrowth and attachment. Presented at 45th Annual Meeting, Orthopedic Research Society, Anaheim, California 1999.
43. Wu W, Nancollas GH. Nucleation and crystal growth of octacalcium phosphate on titanium oxide surfaces. *Langmuir* 1997;13:861-865.
44. Shirkhanzadeh M. Electrochemical preparation of bioactive calcium phosphate coatings on porous substrates by the periodic pulse technique. *Journal of Materials Science Letters* 1993;12:16-19.
45. Zhitomirsky I, Gal-Or L. Electrophoretic deposition of hydroxyapatite. *Journal of Materials Science: Materials in Medicine* 1997;8(4):213-219.
46. Zhitomirsky I. Electrophoretic and electrolytic deposition of ceramic coatings on carbon fibers. *Journal of the European Ceramic Society* 1998;18:849-856.
47. Koura N, Tsukamoto T, Shoji H, Hotta T. Preparation of various oxide films by an electrophoretic deposition method: a study of the mechanism. *Japanese Journal of Applied Physics, Part I: Regular Papers and Short Notes* 1995;34(3):1643-1647.
48. Sugiyama S, Takagi A, Tsuzuki K. (Pb, La)(Zr, Ti)O₃ films by multiple electrophoretic deposition/sintering processing. *Japanese Journal of Applied Physics, Part I: Regular Papers and Short Notes* 1991;30:2170-2173.
49. Shirkhanzadeh M. Direct formation of nanophase hydroxyapatite on cathodically polarized electrodes. *Journal of Materials Science: Materials in Medicine* 1998; 9:67-72.
50. Ban S, Maruno S. Morphology and microstructure of electrochemically deposited calcium phosphates in a modified simulated body fluid. *Biomaterials* 1998; 19(14):1245-1253.

51. Ban S, Maruno S. Deposition of calcium phosphate on titanium by electrochemical process in simulated body fluid. *Japanese Journal of Applied Physics, Part II: Letters* 1993;32:1577-1580.
52. Shirkhazadeh M. Hydroxyapatite particles prepared by electrocrystallization from aqueous electrolytes. *Materials Letters* 1993;15(5-6):392-395.
53. Shirkhazadeh M, inventor; Queen's University at Kingston, assignee. Method for depositing bioactive coatings on conductive substrates. United States patent 5205921. 1993 April 27.
54. Shirkhazadeh M. X-ray diffraction and Fourier transform infrared analysis of nanophase apatite coatings prepared by electrocrystallization. *Nanostructured Materials* 1994;4(6):677-684.
55. Campbell AA, Fryxell GE, Linehan JC, Graff GC. Surface-induced mineralization: A new method for producing calcium phosphate coatings. *Journal of Biomedical Materials Research* 1996;32:111-118.
56. Linde A, Lussi A, Crenshaw MA. Mineral induction by immobilized polyanionic proteins. *Calcified Tissue International* 1989;44:286-295.
57. Kilpadi DV, Lemons JE. Surface energy characterization of unalloyed titanium implants. *Journal of Biomedical Materials Research* 1994;28(12):1419-1425.
58. Kilpadi DV, Raikar GN, Liu J, Lemons JE, Vohra Y, Gregory JC. Effect of surface treatment on unalloyed titanium implants: spectroscopic analyses. *Journal of Biomedical Materials Research* 1998;40(4):646-659.
59. Kilpadi DV, Lemons JE, Liu J, Raikar GN, Weimer JJ, Vohra Y. Cleaning and heat-treatment effects on unalloyed titanium implant surfaces. *International Journal of Oral and Maxillofacial Implants* 2000;15(2):219-230.
60. Hayashi K, Inadome T, Mashima T, Sugioka Y. Comparison of bone-implant interface shear strength of solid hydroxyapatite and hydroxyapatite-coated titanium implants. *Journal of Biomedical Materials Research* 1993;27(5):557-563.
61. Cook SD, Thomas KA, Dalton JF, Volkman TK, Whitecloud TS, Kay JF. Hydroxylapatite coatings of porous implants improves bone ingrowth and interface

- attachment strength. *Journal of Biomedical Materials Research* 1992;26:989-1001.
62. Kumar M, Dasarathy H, Riley C. Electrodeposition of brushite coatings and their transformation to hydroxyapatite in aqueous solutions. *Journal of Biomedical Materials Research* 1999;45(4):302-310.
 63. Han Y, Fu T, Lu J, Xu K. Characterization and stability of hydroxyapatite coatings prepared by an electrodeposition and alkaline-treatment process. *Journal of Biomedical Materials Research* 2001;54(1):96-101.
 64. Yang CY, Lin RM, Wang BC, Lee TM, Chang E, Hang YS, Chen PQ. *In vitro* and *in vivo* mechanical evaluations of plasma-sprayed hydroxyapatite coatings on titanium implants: the effect of coating characteristics. *Journal of Biomedical Materials Research* 1997;37(3):335-345.
 65. Pereira MM, Clark AE, Hench LL. Effect of texture on the rate of hydroxyapatite formation on gel-silica surface. *Journal of the American Ceramic Society* 1995; 78(9):2463-2468.
 66. Li P, Ohtsuki C, Kokubo T. Process of formation of bone-like apatite layer on silica gel. *Journal of Materials Science: Materials in Medicine* 1993;4:127-131.
 67. Li P, Ducheyne P. Quasi-biological apatite film induced by titanium in a simulated body fluid. *Journal of Biomedical Materials Research* 1998;41(3):341-348.
 68. Anselme K. Osteoblast adhesion on biomaterials. *Biomaterials* 2000;21(7):667-681.
 69. Anselme K, Bigerelle M, Noel B, Dufresne E, Judas D, Iost A, Hardouin P. Qualitative and quantitative study of human osteoblast adhesion on materials with various surface roughnesses. *Journal of Biomedical Materials Research* 2000; 49(2):155-166.
 70. Giancotti FG, Ruoslahti E. Integrin signaling. *Science* 1999;285(5430):1028-1032.

71. Bagambisa FB, Joos U, Schilli W. Mechanisms and structure of the bond between bone and hydroxyapatite. *Journal of Biomedical Materials Research* 1993;27: 1047-1055.
72. Kilpadi KL, Chang PL, Bellis SL. Hydroxylapatite binds more serum proteins, purified integrins, and osteoblast precursor cells than titanium or steel. *Journal of Biomedical Materials Research* 2001;57(2):258-267.
73. Ebrahimpour A, Nancollas GH. KS2.bas. Buffalo, NY; 1986.
74. Paunovic M, Schlesinger M, Weil R. Fundamental Considerations. In: Schlesinger M, Paunovic M, editors. *Modern Electroplating*, Fourth Edition. New York: John Wiley & Sons, Inc.; 2000. p 1-60.
75. Lin S, LeGeros RZ, LeGeros JP. Adherent octacalciumphosphate coating on titanium alloy using modulated electrochemical deposition method. *Journal of Biomedical Materials Research* 2003;66A:819-828.
76. Schuhmann W, Kranz C, Wohlschlager H, Strohmeier J. Pulse technique for the electrochemical deposition of polymer films on electrode surfaces. *Biosensors and Bioelectronics* 1997;12(12):1157-1167.

**GRADUATE SCHOOL
UNIVERSITY OF ALABAMA AT BIRMINGHAM
DISSERTATION APPROVAL FORM
DOCTOR OF PHILOSOPHY**

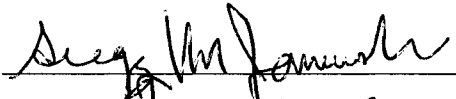
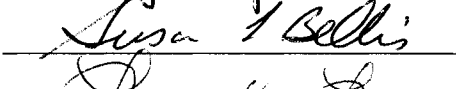
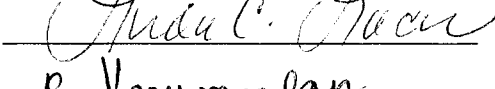
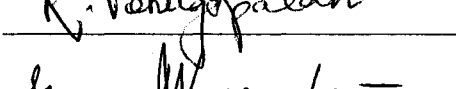
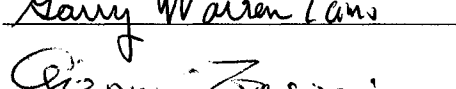
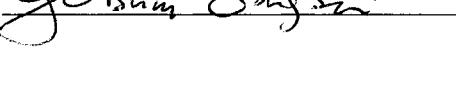
Name of Candidate Rebecca Shumate O'Connor Davis

Graduate Program Materials Science

Title of Dissertation Electrolytic Deposition of Calcium Phosphates on
Modified Titanium Substrates

I certify that I have read this document and examined the student regarding its content. In my opinion, this dissertation conforms to acceptable standards of scholarly presentation and is adequate in scope and quality, and the attainments of this student are such that she may be recommended for the degree of Doctor of Philosophy.

Dissertation Committee:

Name	Signature
<u>Gregg M. Janowski</u> , Chair	
<u>Susan L. Bellis</u>	
<u>Linda C. Lucas</u>	
<u>Ramakrishna Venugopalan</u>	
<u>Garry Warren</u>	
<u>Giovanni Zangari</u>	

Director of Graduate Program

Dean, UAB Graduate School

Date _____

